Trajectory Tracking with Prescribed Performance for Underactuated Underwater Vehicles under Model Uncertainties and External Disturbances

Charalampos P. Bechlioulis, George C. Karras, Shahab Heshmati-alamdari and Kostas J. Kyriakopoulos

***Abstract*—This paper addresses the tracking control problem of 3D trajectories for underactuated underwater robotic vehicles. Our recent theoretical results on the prescribed performance control of fully-actuated nonlinear systems [1], [2] are innovatively extended on the control of the most common types of underactuated underwater vehicles, namely the torpedo-like (i.e., vehicles actuated only in surge, pitch and yaw) and the unicycle-like (i.e., vehicles actuated only in surge, heave and yaw). The main contributions of this work concentrate on: i) the reduced design complexity, ii) the increased robustness against system uncertainties, iii) the prescribed transient and steady state performance as well as iv) the minimal tracking information requirements. More specifically, two smooth control schemes are designed, without any a priori knowledge of the vehicle's dynamic model parameters, that guarantee bounded closed loop signals and tracking with prescribed transient and steady state performance, despite the presence of external disturbances representing ocean currents and waves. Furthermore, only the desired trajectory and none of its higher order derivatives is employed in the control schemes, involving thus applications where the desired trajectory is not a priori known for all time but it is evaluated online and hence its time derivatives are not available. Moreover, the proposed control schemes are of low complexity and can be easily integrated on embedded control platforms with limited power and computational resources (e.g., Autonomous Underwater Vehicles - AUVs). Additionally, the stability of the unactuated degrees of freedom is assured without incorporating the corresponding velocity measurements in the control schemes, thus increasing greatly the robustness against noises that corrupt the specific measurements and simplifying further the implementation. Finally, through the appropriate selection of certain designer-specified performance functions, the proposed schemes efficiently avoid both controllability and representation singularities that inherently arise during the kinematic control design of underactuated vehicles. A comparative simulation study points out the intriguing performance properties of the proposed method, whilst its applicability is experimentally verified using a small unicycle-like underactuated underwater vehicle in a test tank.**

***Index Terms*—Underactuated Underwater Vehicles; Robust Tracking Control; Prescribed Performance Control.**

I. Introduction

UNDERWATER activities have steadily grown in the last fifty years imposing new challenges on technical and engineering researchers supporting the offshore industry growth. Complex inspections of oil/gas subsea pipelines, risers, exploitation rings and novel operations in geological exploration are now required, with the ultimate objective of educing efficiently the plentiful underwater resources. Additionally, a multitude of other non profitable underwater applications in the fields of oceanography, environmental monitoring and marine archeology have recently emerged.

In the recent wake of rapid progress in marine robotics, that affords numerous advanced tools for offshore activities, underwater vehicles have particularly received considerable attention. However, further work remains to be done before underwater robots roam the ocean freely. In that sense, the motion control problem of underwater vehicles continues to pose considerable challenges to system designers in view of the increasingly demanding missions envisioned for underwater robots, especially in the presence of underactuated dynamics, stringent environmental constraints and large model uncertainties.

A typical motion control problem is trajectory tracking that is concerned with the design of control laws that force a vehicle to reach and follow a reference trajectory. Classical approaches such as local linearization and input-output decoupling have been used in the past to design tracking controllers for underactuated vehicles [3]. Nevertheless, the aforementioned methods yielded poor closed loop performance and the results were local, around only certain selected operating points. An alternative approach involves output feedback linearization [4]–[6], which however is not always possible. Moreover, based on a combined approach involving Lyapunov theory and backstepping, various nonlinear model–based trajectory tracking controllers have been reported during the last two decades [7]–[16]. However, these schemes demand a very accurate knowledge of the vehicle dynamic parameters, which in most cases is quite difficult to obtain. More specifically, in [7] the authors proposed a cascade control strategy that consists of a kinematic control law that aims at tracking a desired trajectory and a dynamical control law, based on the backstepping technique, that tracks the desired velocity control signals. In [8], extending from their previous works in [9], [10], the authors proposed a nonlinear adaptive controller that drives an underactuated underwater vehicle moving on a horizontal plane along a sequence of way points. The controller is designed initially at the kinematic level and subsequently, employing the integrator backstepping technique, is extended to the dynamical model. However, the effect of ocean currents either is assumed to be known or an exponential observer is

The authors are with the Control Systems Laboratory, School of Mechanical Engineering, National Technical University of Athens, Athens 15780, Greece. Emails: {chmpechl, karrasg, shahab, kkyria}@mail.ntua.gr. This work was supported by the EU funded project PANDORA: Persistent Autonomy through learNing, aDaptation, Observation and ReplAnning", FP7-288273, 2012-2014.

adopted for its estimation, thus increasing the design complexity. In [12], the authors developed a trajectory tracking controller based on the integral backstepping technique. Nevertheless, the effect of the second hydrodynamic damping force was ignored. In [13] the authors presented a model based output feedback controller for trajectory tracking with a slender-body underactuated underwater vehicle. In a recent work [14], a position tracking controller for underactuated vehicles moving on a horizontal plane was presented. The authors assumed that the motion of the vehicle is affected by constant, unknown ocean currents and designed an observer to estimate them. However, model uncertainties and time varying sea currents were not considered. In [15], a trajectory tracking controller for underactuated vehicles was designed based on the one-step ahead backstepping technique and the Lyapunov's direct method. In order to avoid the geometric singularities in the kinematic model, a combination of the Euler angles and unit-quaternion representation was adopted. However, even though the effect of sea currents was considered, the inherent uncertainties of the dynamic model were ignored. Finally, a path following and trajectory tracking control scheme for underactuated vehicles was proposed in [16], based on previous work in [17], resulting in a more smooth spatial convergence and a more tight temporal performance.

Uncertainties in the dynamic model of underactuated underwater vehicles have been mainly compensated by adaptive control techniques. In [18], a switching adaptive law is combined with a nonlinear control scheme. In [19] the authors, based on their previous work [20], presented a robust adaptive control strategy for path following for an underactuated vehicle in the presence of external disturbances and model uncertainties. However, the application of the aforementioned control schemes in a real time experiment is questionable, owing to their sensitivity to unknown parameters. On the other hand, experimental results for an adaptive control scheme were presented in [21]. Nevertheless, partial a priori knowledge of the dynamic parameters was requested. Additionally, a hybrid parameter adaptation law, based on switching control theory, was adopted in [22], [23]. However, environmental disturbances and unmodeled dynamics were not considered. Alternatively, sliding mode control theory was also employed in [24]–[29] to deal with model uncertainty in the vehicle's dynamic model. Nonetheless, the main disadvantage of the aforementioned control schemes is the inherent control input chattering that is energy intensive and may result in high frequency dynamics, which is undesirable for underwater applications. Finally, adaptive neural network and fuzzy control schemes that deal with model uncertainties have also been proposed in [30]–[35], exploiting the universal approximation capabilities of neural network and fuzzy system structures. Unfortunately, the aforementioned schemes [30]–[35] inherently introduce certain issues affecting closed loop stability and robustness. Specifically, even though the existence of a closed loop initialization set as well as of control gain values that guarantee closed loop stability can be proven, the problem of proposing an explicit constructive methodology capable of a priori imposing the required stability properties is not addressed. As a consequence, the produced control schemes yield inevitably reduced levels of robustness against modeling imperfections. Moreover, the results are restricted to be local as they are valid only within the compact set where the capabilities of the universal approximators hold. Finally, the introduction of approximating/estimating structures increases the complexity of the proposed control schemes in the sense that extra adaptive parameters have to be updated (i.e., extra nonlinear differential equations have to be solved numerically) and extra calculations have to be conducted to output the control signal, thus making their implementation on embedded control systems difficult.

Despite the recent progress in the tracking control for underactuated underwater vehicles, certain issues still remain open. First, even in case of accurately known vehicle model, external disturbances affect the tracking performance severely, thus making the problem of guaranteeing prescribed transient and steady state performance difficult or impossible in certain situations. Furthermore, the tracking performance deterioration becomes more intense when uncertainty in the vehicle model (which is inevitable) is also present. Moreover, all aforementioned developments require accurate measurements of the vehicle velocities in all degrees of freedom as well as of the velocity (and in some cases the acceleration) of the desired trajectory, which significantly increases the cost of the vehicle's sensor suite and the complexity of the sensor fusion algorithms, thus reducing their applicability.

Contrary to the current state of the art in the underwater vehicle control literature, the proposed control schemes that are designed for the most common types of underactuated underwater vehicles[1], namely torpedo-like and unicycle-like vehicles, achieve tracking with prescribed performance despite the presence of external disturbances representing ocean currents and waves and without requiring prior information of the vehicle's dynamic model parameters. The main contributions of this work can be summarized as follows:

1) Structural Complexity and Robustness against Measurement Noises: The proposed control schemes do not incorporate any prior knowledge of the external disturbances and the vehicle's dynamic model parameters or even of some corresponding upper bounding constants. Furthermore, no estimation (i.e., adaptive control) has been employed to acquire such knowledge. Moreover, compared with the traditional backstepping-like approaches, the proposed schemes prove significantly less complex. No hard calculations are required to output the proposed control signals, thus making implementation straightforward. Finally, no velocity measurements of the unactuated degrees of freedom are incorporated in the control schemes, thus increasing greatly the robustness against noises that corrupt the specific measurements and simplifying further the implementation.

2) Robust Prescribed Performance and Control Gains Selection: The actual tracking performance of the proposed control schemes is solely determined by certain designer specified performance functions and is isolated from the control gains

[1]In this work, we extend our recent results [36] on the control of torpedo-like underwater vehicles by additionally studying the stability of the unactuated degrees of freedom as well as by considering the unicycle-like underactuated model of underwater vehicles.

selection as well as from the model uncertainties, thus extending greatly the robustness of the closed loop system. In this way, the control objectives are achieved without resorting to extreme values of the control gains. Their selection is significantly simplified to adopting those values that lead to reasonable control effort.

3) Minimal Tracking Information: The proposed control schemes are independent of the time derivatives of the desired trajectory. Hence, applications where the desired trajectory is not a priori known for all time but it is measured and thus its time derivatives are not available, can be considered.

A. Preliminaries

At this point, we recall some notations, definitions and preliminary results that are necessary in the subsequent analysis.

1) Notation: Throughout this paper, I_n is the n-th dimensional identity matrix, $\Re^n$ denotes the n-th dimensional Euclidean space and $\Re^{n\times n}$ represents the set of all square $n \times n$ real matrices. The absolute value of a scalar $a \in \Re$ and the Euclidean norm of a vector $\boldsymbol{a} \in \Re^n$ are denoted by $|a|$ and $\|\boldsymbol{a}\|$ respectively. Furthermore, given a positive definite matrix A, $\lambda_{\min}(A)$ and $\lambda_{\max}(A)$ denote its minimum and maximum eigenvalues. Finally, $SO(3) = \left\{A \in \Re^{3\times 3} : AA^T = I_3 \ \& \ \det(A) = 1\right\}$ denotes the group of all normal rotations.

2) Prescribed Performance: It will be clearly demonstrated in the sequel that the concepts and techniques of prescribed performance control, recently developed in [1], [2] for fully-actuated nonlinear systems, are innovatively adapted to deal with the tracking control problem of underactuated underwater vehicles. Prescribed performance characterizes the behavior where the tracking error converges to a predefined arbitrarily small residual set with convergence rate no less than a certain predefined value. In that respect, consider a generic scalar tracking error $e(t)$. Prescribed performance is achieved if $e(t)$ evolves strictly within a predefined region that is bounded by certain functions of time. The mathematical expression of prescribed performance is given by the following inequalities:

$$\rho_L(t) < e(t) < \rho_U(t), \ \forall t \geq 0 \tag{1}$$

where $\rho_L(t)$, $\rho_U(t)$ are smooth and bounded functions of time satisfying $\lim_{t\to\infty}\rho_U(t) > \lim_{t\to\infty}\rho_L(t)$, called performance functions. In this sense, consider the exponential performance functions $\rho_i(t) = (\rho_{i0} - \rho_{i\infty})\exp(-l_i t) + \rho_{i\infty}$ with ρ_{i0}, $\rho_{i\infty}$, l_i, $i \in \{L, U\}$ appropriately chosen constants. Specifically, the constants $\rho_{L0} = \rho_L(0)$, $\rho_{U0} = \rho_U(0)$ are selected such that $\rho_{L0} < e(0) < \rho_{U0}$. Furthermore, the constants $\rho_{L\infty} = \lim_{t\to\infty}\rho_L(t)$, $\rho_{U\infty} = \lim_{t\to\infty}\rho_U(t)$ represent the maximum allowable range of the tracking error $e(t)$ at steady state, which may even be set arbitrarily small to a value reflecting the resolution of the measurement device, thus achieving practical convergence of $e(t)$ to zero. Moreover, the decreasing rate of $\rho_L(t)$, $\rho_U(t)$ which is affected by the constants l_L, l_U in this case, introduces a lower bound on the required speed of convergence of $e(t)$. Therefore, the appropriate selection of the performance functions $\rho_L(t)$, $\rho_U(t)$ imposes transient and steady state performance characteristics on the tracking error $e(t)$.

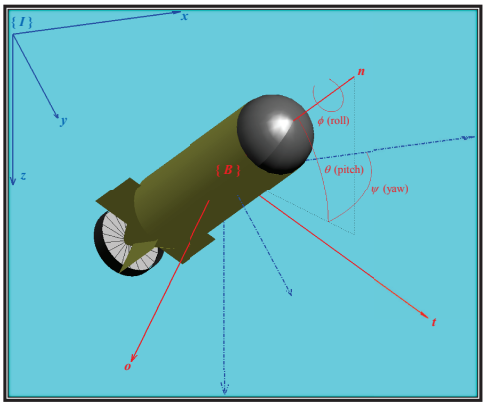

Fig. 1: The inertial (blue) and the body-fixed (red) coordinate frames.

3) Dynamical Systems: In this work, the forward completeness of the closed loop system will be based on the following preliminary results on dynamical systems. Thus, consider the initial value problem:

$$\dot{\xi} = h(t, \xi), \ \xi(0) = \xi^0 \in \Omega_\xi \tag{2}$$

with $h : \Re_+ \times \Omega_\xi \to \Re^n$, where $\Omega_\xi \subset \Re^n$ is a non-empty open set.

Definition 1. *[37] A solution $\xi(t)$ of the initial value problem (2) is maximal if it has no proper right extension that is also a solution of (2).*

Theorem 1. *[37] Consider the initial value problem (2). Assume that $h(t, \xi)$ is: a) locally Lipschitz on ξ for almost all $t \in \Re_+$, b) piecewise continuous on t for each fixed $\xi \in \Omega_\xi$ and c) locally integrable on t for each fixed $\xi \in \Omega_\xi$. Then, there exists a maximal solution $\xi(t)$ of (2) on the time interval $[0, \ \tau_{\max})$ with $\tau_{\max} > 0$ such that $\xi(t) \in \Omega_\xi$, $\forall t \in [0, \ \tau_{\max})$.*

Proposition 1. *[37] Assume that the hypotheses of Theorem 1 hold. For a maximal solution $\xi(t)$ on the time interval $[0, \ \tau_{\max})$ with $\tau_{\max} < \infty$ and for any compact set $\Omega'_\xi \subset \Omega_\xi$ there exists a time instant $t' \in [0, \ \tau_{\max})$ such that $\xi(t') \notin \Omega'_\xi$.*

II. Problem Statement

In this section, the kinematics and dynamics of a 6 DoF underwater vehicle model are initially presented. Subsequently, we introduce two of the most common classes of underactuated vehicles that are considered in this work (i.e., torpedo-like and unicycle-like underactuated vehicles) and finally the trajectory tracking problem is rigorously formulated.

A. Vehicle kinematics and dynamics

Consider a neutrally buoyant underwater vehicle modeled as a rigid body subject to external forces and torques. Let $\{I\}$ be an inertial coordinate frame and $\{B\}$ a body-fixed coordinate frame with orthonormal axes $\boldsymbol{n} = [n_x, n_y, n_z]^T$, $\boldsymbol{o} = [o_x, o_y, o_z]^T$, $\boldsymbol{t} = [t_x, t_y, t_z]^T$ relative to $\{I\}$, whose origin O_B is located at the center of mass of the vehicle (see Fig. 1). Further, let $\mathbf{p} = [x, y, z]^T \in \Re^3$ be the position of O_B in $\{I\}$ and $R = [\boldsymbol{n}, \boldsymbol{o}, \boldsymbol{t}] \in SO(3)$ the rotation matrix that describes the orientation of the vehicle. Let $\mathbf{v} = [u, v, w]^T$ be the linear velocity (u, v, w are the longitudinal-surge,

transverse-sway and vertical-heave velocities along the body frame axis $\boldsymbol{n}$, $\boldsymbol{o}$, $\boldsymbol{t}$ respectively) and $\mathbf{w} = [p, q, r]^T$ be the angular velocity (p, q, r are the angular velocities around the longitudinal-roll, the transverse-pitch and vertical-yaw axis respectively) of O_B with respect to $\{I\}$ expressed in $\{B\}$. Hence, the kinematic equations of motion for the considered vehicle may be written as:

$$\dot{\mathbf{p}} = R\mathbf{v} + \delta_{\mathbf{c}}(t) \tag{3}$$

$$\dot{R} = RS(\mathbf{w}) \tag{4}$$

where $\delta_{\mathbf{c}}(t) = [\delta_x(t), \delta_y(t), \delta_z(t)]^T$ denotes bounded and slowly varying ocean currents [3] and $S(\mathbf{w}) = \begin{bmatrix} 0 & -r & q \\ r & 0 & -p \\ -q & p & 0 \end{bmatrix}$. Alternatively, the orientation of the vehicle may be described by the Euler angles' parameterization $\boldsymbol{\eta} = [\phi, \theta, \psi]^T$, where ϕ, θ and ψ are the roll, pitch, yaw angles respectively, that is mainly employed owing to its physical meaning (i.e., the inertial coordinate frame $\{I\}$ after three successive rotations of ψ, θ, ϕ angles about its z, y and x axes respectively ends up parallel to the body-fixed coordinate frame $\{B\}$, see Fig. 1). Thus, the rotation matrix R may be expressed via the roll, pitch and yaw angles as follows:

$$R(\boldsymbol{\eta}) = \begin{bmatrix} \mathrm{c}_\psi \mathrm{c}_\theta & \mathrm{c}_\psi \mathrm{s}_\theta \mathrm{s}_\phi - \mathrm{s}_\psi \mathrm{c}_\phi & \mathrm{c}_\psi \mathrm{s}_\theta \mathrm{c}_\phi + \mathrm{s}_\psi \mathrm{s}_\phi \\ \mathrm{s}_\psi \mathrm{c}_\theta & \mathrm{s}_\psi \mathrm{s}_\theta \mathrm{s}_\phi + \mathrm{c}_\psi \mathrm{c}_\phi & \mathrm{s}_\psi \mathrm{s}_\theta \mathrm{c}_\phi - \mathrm{c}_\psi \mathrm{s}_\phi \\ -\mathrm{s}_\theta & \mathrm{c}_\theta \mathrm{s}_\phi & \mathrm{c}_\theta \mathrm{c}_\phi \end{bmatrix} \tag{5}$$

where $\mathrm{s}_\star = \sin(\star)$ and $\mathrm{c}_\star = \cos(\star)$. Additionally, the body-fixed angular velocity $\mathbf{w}$ and the Euler angles' rate $\dot{\boldsymbol{\eta}}$ are related through $\dot{\boldsymbol{\eta}} = J(\boldsymbol{\eta})\mathbf{w}$ where:

$$J(\boldsymbol{\eta}) = \begin{bmatrix} 1 & \mathrm{t}_\theta \mathrm{s}_\phi & \mathrm{t}_\theta \mathrm{c}_\phi \\ 0 & \mathrm{c}_\phi & -\mathrm{s}_\phi \\ 0 & \mathrm{s}_\phi / \mathrm{c}_\theta & \mathrm{c}_\phi / \mathrm{c}_\theta \end{bmatrix} \tag{6}$$

is a transformation matrix that does not belong to $SO(3)$ (i.e., $J^T(\boldsymbol{\eta}) \neq J^{-1}(\boldsymbol{\eta})$) with $\mathrm{t}_\star = \tan(\star)$. In this way, the kinematic equations of the vehicle may be written in the Euler angles' representation as follows:

$$\dot{\mathbf{p}} = R(\boldsymbol{\eta})\mathbf{v} + \delta_{\mathbf{c}}(t) \tag{7}$$

$$\dot{\boldsymbol{\eta}} = J(\boldsymbol{\eta})\mathbf{w} \tag{8}$$

where $R(\boldsymbol{\eta})$ and $J(\boldsymbol{\eta})$ are defined in (5) and (6) respectively.

Under standard simplifications owing to symmetries in the mass configuration [3], the dynamic equations of motion of underwater vehicles may be written as:

$$m_u \dot{u} = m_v v r - m_w w q + X_u u + X_{|u|u} |u| u + X + \delta_u(t) \tag{9}$$

$$m_v \dot{v} = m_w w p - m_u u r + Y_v v + Y_{|v|v} |v| v + Y + \delta_v(t) \tag{10}$$

$$m_w \dot{w} = m_u u q - m_v v p + Z_w w + Z_{|w|w} |w| w + Z + \delta_w(t) \tag{11}$$

$$m_p \dot{p} = m_{vw} v w + m_{qr} q r + K_p p + K_{|p|p} |p| p + z_B W \mathrm{c}_\theta \mathrm{s}_\phi + K + \delta_p(t) \tag{12}$$

$$m_q \dot{q} = m_{wu} w u + m_{rp} r p + M_q q + M_{|q|q} |q| q + z_B W \mathrm{s}_\theta + M + \delta_q(t) \tag{13}$$

$$m_r \dot{r} = m_{uv} u v + m_{pq} q q + N_r r + N_{|r|r} |r| r + N + \delta_r(t) \tag{14}$$

where m_u, m_v, m_w, m_p, m_q, m_r denote the vehicle's mass/moment of inertia and added mass/moment of inertia with $m_{vw} = m_v - m_w$, $m_{wu} = m_w - m_u$, $m_{uv} = m_u - m_v$, $m_{qr} = m_q - m_r$, $m_{rp} = m_r - m_p$, $m_{pq} = m_p - m_q$ and X_u, $X_{|u|u}$, Y_v, $Y_{|v|v}$, Z_w, $Z_{|w|w}$, K_p, $K_{|p|p}$, M_q, $M_{|q|q}$, N_r, $N_{|r|r}$ are negative hydrodynamic damping coefficients. It is also assumed that the vehicle's center of buoyancy lies on the body-fixed z-axis (i.e., heave) above its center of gravity (i.e., $z_B < 0$ where z_B defines the position of the center of buoyancy[2] with respect to O_B). Moreover, $\delta_u(t)$, $\delta_v(t)$, $\delta_w(t)$, $\delta_p(t)$, $\delta_q(t)$, $\delta_r(t)$ denote bounded exogenous forces and torques acting on surge, sway, heave, roll, pitch, yaw owing to ocean waves [3] and X, Y, Z, K, M, N denote (depending on the vehicle's degrees of actuation as discussed in the sequel) control input forces and torques that are applied in order to produce the desired motion of the body fixed frame.

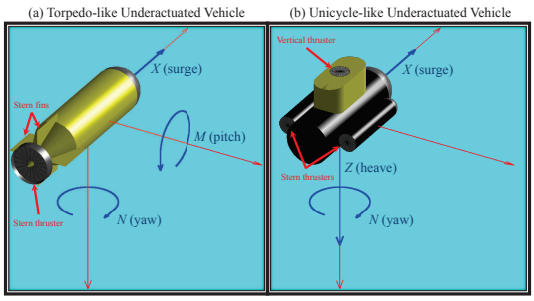

Fig. 2: The main classes of underactuated underwater vehicles. Blue color indicates the actuated degrees of freedom.

B. Classes of underactuated vehicles

In this work, we consider the most common types of underactuated underwater vehicles, namely the torpedo-like and unicycle-like vehicles (see Fig. 2).

Torpedo-like underactuated vehicles: The vehicles considered in this class are actuated by a force X along their longitudinal (surge) axis as well as by torques M and N about their transverse (pitch) and vertical (yaw) axes respectively (see Fig. 2a). The aforementioned force X and torques M, N define the input control variables of the corresponding dynamic system (9)-(14), which in this case is unactuated in sway, heave and roll degrees of freedom (i.e., $Y = 0$, $Z = 0$ and $K = 0$).

Unicycle-like underactuated vehicles: The vehicles considered in this class are actuated by forces X and Z along the longitudinal (surge) and vertical (heave) axes respectively and a torque N about the vertical (yaw) axis (see Fig. 2b). The aforementioned forces X, Z and torque N define the input control variables of the corresponding dynamic system (9)-(14), which in this case is unactuated in sway, roll and pitch degrees of freedom (i.e., $Y = 0$, $K = 0$ and $M = 0$).

Remark 1. *Torpedo-like vehicles are commonly equipped with only one stern thruster and two stern fins (see Fig. 2a). In this way, the action of the stern thruster results in force X and the pitch and yaw moments M, N satisfy:*

$$M \propto u^2 \delta_q,\ N \propto u^2 \delta_r \tag{15}$$

where u is the surge velocity and δ_q, δ_r denote the angles of the corresponding fins. In addition, unicycle-like vehicles are

[2]Notice that the vehicle weight W is equal to the buoyancy force, owing to the neutral buoyancy assumption.

usually equipped with two identical rear thrusters, mounted symmetrically with respect to their longitudinal axis as well as a thruster mounted along the vertical axis (see Fig. 2b). In this way, the common and the differential action modes of the rear thrusters result in force X and torque N respectively, whereas the action of the vertical thruster results in force Z. However, the control input signals, that will be designed in the sequel for both cases, are forces and torques exerted at the center of mass of the vehicle (which is a common practice in the related literature as well), and not direct commands to the vehicle actuators (i.e, thrusters' commands and fins' angles). Hence, dealing with potential uncertainties within the mapping between desired body forces/torques and actuator commands is left for future investigation.

Remark 2. *Despite its physical meaning, Euler angles' parameterization introduces a representation singularity in (8), when the pitch angle θ approaches $\pm 90^o$. In this respect, since torpedo-like vehicles may operate close to this singularity, our approach for this class will be based on the rotation matrix parameterization that does not suffer from geometric singularities. On the other hand, for the class of unicycle-like underactuated vehicles, since the unactuated pitch degree of freedom is passive (i.e., the pitch angle will be proven to remain bounded close to zero), the Euler angles' parameterization will be adopted for the clarity of presentation.*

C. Control objective

Let $\boldsymbol{p}_d(t) = [x_d(t), y_d(t), z_d(t)]^T$ denote a smooth desired trajectory with bounded time derivatives (i.e., a trajectory with bounded velocity, acceleration, etc.). The objective of this paper is to propose robust control laws for the aforementioned classes of underactuated vehicles that track the desired trajectory $\boldsymbol{p}_d(t)$ with prescribed performance, regarding the steady state error and the speed of convergence (see Subsection I-A2), despite the presence of exogenous disturbances representing ocean currents and waves. Hence, the problem treated in this work reads as follows:

Problem (Robust Prescribed Performance Tracking Control for Underactuated Underwater Vehicles): Design approximation-free control schemes for torpedo-like and unicycle-like underactuated underwater vehicles with dynamic model uncertainty, such that all signals in the closed loop system remain bounded and moreover the desired trajectory $\boldsymbol{p}_d(t)$ is tracked with prescribed transient and steady state performance.

Remark 3. *In this work and contrary to what is common practice in the related literature, no prior knowledge of the vehicle dynamic parameters and external disturbances or even of some corresponding upper bounding constants will be incorporated in the control design. Furthermore, no estimation (i.e., adaptive control techniques) will be employed to acquire such knowledge, thus reducing the computational complexity significantly and hence making implementation straightforward and efficient on embedded control platforms of autonomous underwater vehicles, endowed with limited power and computational resources.*

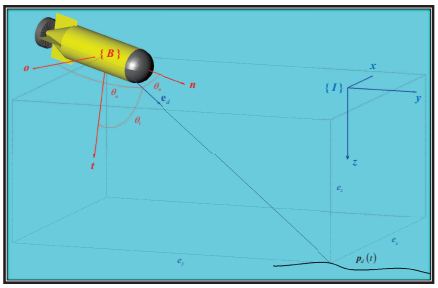

Fig. 3: Torpedo-like vehicle: Graphical illustration of the error definition.

III. Control Design

In this section, we shall present two model-free control schemes of low-complexity, for torpedo-like and unicycle-like underactuated underwater vehicles respectively, that lead to the solution of the robust prescribed performance tracking control problem stated in the previous section.

A. Torpedo-like underactuated vehicles

Given the desired trajectory $\boldsymbol{p}_d(t) = [x_d(t), y_d(t), z_d(t)]^T$, let us define the distance error:

$$e_d = \sqrt{e_x^2 + e_y^2 + e_z^2}, \tag{16}$$

where

$$e_x = x_d(t) - x,\ e_y = y_d(t) - y,\ e_z = z_d(t) - z, \tag{17}$$

as well as the orientation errors:

$$e_t = \frac{e_x}{e_d} t_x + \frac{e_y}{e_d} t_y + \frac{e_z}{e_d} t_z \triangleq \mathrm{c}_{\theta_t}, \tag{18}$$

$$e_o = \frac{e_x}{e_d} o_x + \frac{e_y}{e_d} o_y + \frac{e_z}{e_d} o_z \triangleq \mathrm{c}_{\theta_o}, \tag{19}$$

where θ_t, θ_o are the angles measured from the unit error vector $\mathbf{e}_d \triangleq \left[\frac{e_x}{e_d}, \frac{e_y}{e_d}, \frac{e_z}{e_d}\right]^T$ to the transverse $\boldsymbol{o} = [o_x, o_y, o_z]^T$ and vertical $\boldsymbol{t} = [t_x, t_y, t_z]^T$ axis of the vehicle respectively. Eqs. (18) and (19) can be easily verified if we consider the inner products of the unit vector $\mathbf{e}_d$ with the unit vectors of the transverse $\boldsymbol{o}$ and vertical $\boldsymbol{t}$ axis respectively, which equal to the cosine of the angles defined by the corresponding vectors (see Fig. 3). It should be noted that the aforementioned error transformations (16)-(19) are employed to display the vehicle kinematics in a form that greatly helps motivate the structure of the controller derived in the sequel. Hence, the tracking control problem is solved if the distance error e_d and the orientation errors e_t, e_o reduce to zero (i.e., the vehicle is heading to the desired trajectory, since the unit vector $\mathbf{e}_d$ tends to be normal to both the transverse $\boldsymbol{o}$ and vertical $\boldsymbol{t}$ axis of the vehicle and consequently aligned to its longitudinal $\boldsymbol{n}$ axis, when $e_t \to 0$ and $e_o \to 0$). However, notice from (18) and (19) that the orientation errors e_t, e_o are well-defined only for nonzero values of e_d, since the angles θ_t, θ_o are unidentified when $e_d = 0$[3]. Thus, the proposed control scheme will be designed to further guarantee that $e_d(t) > \underline{\rho}_d > 0$, $\forall t \geq 0$, for an arbitrarily small positive design constant $\underline{\rho}_d$, in order to avoid the aforementioned singularity issue when $e_d \to 0$.

[3]Notice that the error vector $\mathbf{e}_d$ tends to the origin in such case. Hence, the angles θ_t, θ_o cannot be defined appropriately.

Differentiating (16)-(19) and employing (3), (4) to obtain the kinematics of the vehicle in the aforementioned error coordinates, we arrive at:

$$\dot{e}_d = -u\mathrm{c}_{\theta_n} - v\mathrm{c}_{\theta_o} - w\mathrm{c}_{\theta_t} + \frac{e_x(\dot{x}_d-\delta_x)+e_y\left(\dot{y}_d-\delta_y\right)+e_z(\dot{z}_d-\delta_z)}{e_d}, \tag{20}$$

$$\dot{e}_t = q\mathrm{c}_{\theta_n} - p\mathrm{c}_{\theta_o} + \frac{u\mathrm{c}_{\theta_n}\mathrm{c}_{\theta_t}+v\mathrm{c}_{\theta_o}\mathrm{c}_{\theta_t}-w\mathrm{s}^2_{\theta_t}}{e_d} + \frac{(\dot{x}_d-\delta_x)\left(e_d t_x+e_x\mathrm{c}_{\theta_t}\right)}{e_d^2} + \frac{\left(\dot{y}_d-\delta_y\right)\left(e_d t_y+e_y\mathrm{c}_{\theta_t}\right)}{e_d^2} + \frac{(\dot{z}_d-\delta_z)\left(e_d t_z+e_z\mathrm{c}_{\theta_t}\right)}{e_d^2}, \tag{21}$$

$$\dot{e}_o = -r\mathrm{c}_{\theta_n} + p\mathrm{c}_{\theta_t} + \frac{u\mathrm{c}_{\theta_n}\mathrm{c}_{\theta_o}-v\mathrm{s}^2_{\theta_o}+w\mathrm{c}_{\theta_t}\mathrm{c}_{\theta_o}}{e_d} + \frac{(\dot{x}_d-\delta_x)\left(e_d o_x+e_x\mathrm{c}_{\theta_o}\right)}{e_d^2} + \frac{\left(\dot{y}_d-\delta_y\right)\left(e_d o_y+e_y\mathrm{c}_{\theta_o}\right)}{e_d^2} + \frac{(\dot{z}_d-\delta_z)\left(e_d o_z+e_z\mathrm{c}_{\theta_o}\right)}{e_d^2}, \tag{22}$$

where the following equality:

$$\tfrac{e_x}{e_d}n_x + \tfrac{e_y}{e_d}n_y + \tfrac{e_z}{e_d}n_z \triangleq \mathrm{c}_{\theta_n}$$

has been utilized, with θ_n denoting the angle measured from the vector $\mathbf{e}_d$ to the longitudinal $\boldsymbol{n} = [n_x, n_y, n_z]^T$ axis of the vehicle. Finally, to solve the robust prescribed performance tracking control problem, we pose the following assumption.

Assumption 1. *The initial position error $e_d(0)$ and heading angle $\theta_n(0)$ satisfy: a) $e_d(0) > \underline{\rho}_d$ and b) $|\theta_n(0)| < \frac{\pi}{2}$ for an arbitrarily small positive design constant $\underline{\rho}_d$.*

Remark 4. *Assumption 1 guarantees via (a) that the orientation errors e_t, e_o are initially well-defined as well as via (b) that (20)-(22) are initially controllable since $|\theta_n(0)| = \frac{\pi}{2}$ (i.e., $c_{\theta_n(0)} = 0$) renders them initially uncontrollable with respect to u, q and r respectively. In this respect, we shall design a controller that, besides guaranteeing $e_d(t) > \underline{\rho}_d > 0$, $\forall t \geq 0$, further forces the heading angle θ_n to satisfy $|\theta_n(t)| \leq \bar{\theta}_n < \frac{\pi}{2}$, $\forall t \geq 0$ for a positive constant $\bar{\theta}_n$, thus evolving away from the aforementioned uncontrollable point. Finally, notice from a practical point of view that Assumption 1 can be easily enforced by simply placing the vehicle in an initial configuration that is heading towards the desired trajectory (target), which is quite reasonable in underwater applications.*

Control Scheme: The proposed control scheme is first derived at the kinematic level assuming that the control signals are the surge velocity u as well as the pitch and yaw angular velocities q, r. Subsequently, the kinematic controller is extended to the dynamic model, considering the actual control input signals X, M, and N (i.e., a force X in surge and torques M, N in pitch and yaw). Hence, given a smooth desired trajectory $\boldsymbol{p}_d(t) = [x_d(t), y_d(t), z_d(t)]^T$ with bounded time derivatives, and any initial vehicle configuration satisfying Assumption 1 for an arbitrarily small positive design constant $\underline{\rho}_d$, the proposed control design is:

Kinematic Controller: *Select position/orientation performance functions $\rho_d(t)$, $\rho_t(t)$, $\rho_o(t)$ that i) satisfy:*

a_{kin}	$e_d(0) < \rho_d(0)$	$\underline{\rho}_d < \rho_d(t)$	$\underline{\rho}_d < \lim_{t\to\infty} \rho_d(t)$
b_{kin}	$\lvert e_t(0)\rvert < \rho_t(0) < 1$	$0 < \rho_t(t)$	$0 < \lim_{t\to\infty} \rho_t(t)$
c_{kin}	$\lvert e_o(0)\rvert < \rho_o(0) < 1$	$0 < \rho_o(t)$	$0 < \lim_{t\to\infty} \rho_o(t)$
d_{kin}	$\rho_o^2(t) + \rho_t^2(t) \leq \bar{\rho} < 1$, $\forall t \geq 0$		

for a positive constant $\bar{\rho} < 1$ and ii) incorporate the desired performance specifications regarding the steady state error and the speed of convergence (see Subsection I-A2). Subsequently, design the desired velocities:

$$u_d = k_d \ln\left(\frac{1+\frac{e_d-\frac{\rho_d(t)+\underline{\rho}_d}{2}}{\frac{\rho_d(t)-\underline{\rho}_d}{2}}}{1-\frac{e_d-\frac{\rho_d(t)+\underline{\rho}_d}{2}}{\frac{\rho_d(t)-\underline{\rho}_d}{2}}}\right) \tag{23}$$

$$q_d = -k_t \ln\left(\frac{1+\frac{e_t}{\rho_t(t)}}{1-\frac{e_t}{\rho_t(t)}}\right) \tag{24}$$

$$r_d = k_o \ln\left(\frac{1+\frac{e_o}{\rho_o(t)}}{1-\frac{e_o}{\rho_o(t)}}\right) \tag{25}$$

with positive control gains k_d, k_t, k_o.

Dynamic Controller: *Select velocity performance functions $\rho_u(t)$, $\rho_q(t)$, $\rho_r(t)$ that satisfy:*

a_{dyn}	$\lvert u(0) - u_d(0)\rvert < \rho_u(0)$	$0 < \rho_u(t)$	$0 < \lim_{t\to\infty} \rho_u(t)$
b_{dyn}	$\lvert q(0) - q_d(0)\rvert < \rho_q(0)$	$0 < \rho_q(t)$	$0 < \lim_{t\to\infty} \rho_q(t)$
c_{dyn}	$\lvert r(0) - r_d(0)\rvert < \rho_r(0)$	$0 < \rho_r(t)$	$0 < \lim_{t\to\infty} \rho_r(t)$

and design the force in the surge as well as the torques in pitch and yaw as:

$$X = -k_u \ln\left(\frac{1+\frac{u-u_d}{\rho_u(t)}}{1-\frac{u-u_d}{\rho_u(t)}}\right) \tag{26}$$

$$M = -k_q \ln\left(\frac{1+\frac{q-q_d}{\rho_q(t)}}{1-\frac{q-q_d}{\rho_q(t)}}\right) \tag{27}$$

$$N = -k_r \ln\left(\frac{1+\frac{r-r_d}{\rho_r(t)}}{1-\frac{r-r_d}{\rho_r(t)}}\right) \tag{28}$$

with positive control gains k_u, k_q, k_r.

We now summarize the main results of this subsection in the following theorem.

Theorem 2. *Consider any smooth desired trajectory $\boldsymbol{p}_d(t) = [x_d(t), y_d(t), z_d(t)]^T$ with bounded derivatives and a torpedo-like underactuated underwater vehicle modeled by (3), (4) and (9)-(14) in any initial configuration satisfying Assumption 1, for an arbitrarily small positive design constant $\underline{\rho}_d$. The proposed control scheme (23)-(28) guarantees:*

$$\left.\begin{array}{r} \underline{\rho}_d < e_d(t) < \rho_d(t) \\ -\rho_t(t) < e_t(t) < \rho_t(t) \\ -\rho_o(t) < e_o(t) < \rho_o(t) \end{array}\right\}, \forall t \geq 0$$

for appropriately selected performance functions $\rho_d(t)$, $\rho_t(t)$, $\rho_o(t)$ that incorporate the desired transient and steady state performance specifications, and avoids the singularities introduced by the error transformation (16)-(19) with bounded closed loop signals, thus leading to the solution of the robust prescribed performance tracking control problem as stated in Subsection II-C.

Proof. *See the Appendix.*

Remark 5. *Initially, based on Assumption 1, the orientation errors e_t, e_o are well-defined and Eqs. (20)-(22) are controllable. Subsequently, the performance functions $\rho_d(t)$, $\rho_t(t)$ and $\rho_o(t)$ are selected such that the orientation errors are retained well defined and the controllability of (20)-(22) is preserved as long as prescribed performance is guaranteed, that is $\underline{\rho}_d < e_d(t) < \rho_d(t)$, $-\rho_o(t) < e_o(t) < \rho_o(t)$, $-\rho_t(t) < e_t(t) < \rho_t(t)$, $\forall t \geq 0$. Due to property-d_{kin} (i.e., $\rho_o^2(t) + \rho_t^2(t) \leq \bar{\rho} < 1$) the prescribed performance guarantees lead to $e_o^2(t)+e_t^2(t) = c_{\theta_o(t)}^2 + c_{\theta_t(t)}^2 = 1 - c_{\theta_{n_t}(t)}^2 \leq \rho_o^2(t) + \rho_t^2(t) \leq \bar{\rho}$ and consequently to $|\theta_n(t)| < \bar{\theta}_n = \cos^{-1}\left(\sqrt{1-\bar{\rho}}\right) < \frac{\pi}{2}$, $\forall t \geq 0$. Hence, the satisfaction of prescribed performance constitutes a sufficient condition for bypassing the aforementioned singularity issues.*

B. Unicycle-like underactuated vehicles

Given the desired trajectory $\boldsymbol{p}_d(t) = [x_d(t), y_d(t), z_d(t)]^T$, let us define the position errors:

$$e_x = x_d(t) - x,\ e_y = y_d(t) - y,\ e_z = z_d(t) - z, \tag{29}$$

the projected on the horizontal plane distance error:

$$e_d = \sqrt{e_x^2 + e_y^2} \tag{30}$$

as well as the projected on the horizontal plane orientation error:

$$e_o = \frac{e_x}{e_d}\mathrm{s}_\psi - \frac{e_y}{e_d}\mathrm{c}_\psi = \mathrm{s}_{\psi_e}, \tag{31}$$

where ψ is the yaw angle and ψ_e is the angle measured from the normalized error vector $\mathbf{e}_d := \left[\frac{e_x}{e_d}, \frac{e_y}{e_d}, 0\right]^T$ on the horizontal plane to the normalized projection of the longitudinal axis of the vehicle on the horizontal plane, defined by the vector $[\mathrm{c}_\psi, \mathrm{s}_\psi, 0]^T$. Eq. (31) can be easily verified if we consider the cross product of the unit vectors $\mathbf{e}_d$ and $[\mathrm{c}_\psi, \mathrm{s}_\psi, 0]^T$, which equals to the sine of the angle the aforementioned vectors define (see Fig.4). It should be noted that the aforementioned error transformations (29)-(31) are employed to display the vehicle kinematics in a form that greatly helps motivate the structure of the controller derived in the sequel. Hence, the tracking control problem is solved if the projected on the horizontal plane distance error e_d, the vertical error e_z and the orientation error e_o reduce to zero (i.e., the vehicle is heading to the desired trajectory since the unit vector $\mathbf{e}_d$ tends to be aligned with the longitudinal axis of the vehicle, when $e_z \to 0$ and $e_o \to 0$). However, notice from (31) that the orientation error e_o is well-defined only for nonzero values of e_d, since the angle ψ_e is unidentified when $e_d = 0$[4]. Thus, the proposed control scheme will be designed to further guarantee that $e_d(t) > \underline{\rho}_d > 0$, $\forall t \geq 0$, for an arbitrarily small positive design constant $\underline{\rho}_d$, in order to avoid the aforementioned singularity issue when $e_d \to 0$.

Differentiating (29)-(31) and employing (5)-(8) to obtain the kinematics of the vehicle in the aforementioned error coordinates, we arrive at:

[4]Notice that the error vector $\mathbf{e}_d$ tends to the origin in such case. Hence, the angle ψ_e cannot be defined appropriately.

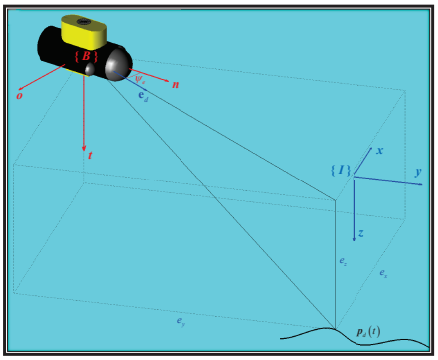

Fig. 4: Unicycle-like vehicle: Graphical illustration of the error definition.

$$\dot{e}_d = -u\mathrm{c}_{\psi_e}\mathrm{c}_\theta - v\left(\mathrm{c}_{\psi_e}\mathrm{s}_\theta\mathrm{s}_\phi - \mathrm{s}_{\psi_e}\mathrm{c}_\phi\right) - w\left(\mathrm{c}_{\psi_e}\mathrm{s}_\theta\mathrm{c}_\phi + \mathrm{s}_{\psi_e}\mathrm{s}_\phi\right) + \left(\dot{x}_d(t) - \delta_x(t)\right)\mathrm{c}_{\psi-\psi_e} + \left(\dot{y}_d(t) - \delta_y(t)\right)\mathrm{s}_{\psi-\psi_e}, \tag{32}$$

$$\dot{e}_z = u\mathrm{s}_\theta - v\mathrm{c}_\theta\mathrm{s}_\phi - w\mathrm{c}_\theta\mathrm{c}_\phi + \dot{z}_d(t) - \delta_z(t), \tag{33}$$

$$\dot{e}_o = q\mathrm{c}_{\psi_e}\frac{\mathrm{s}_\phi}{\mathrm{c}_\theta} + r\mathrm{c}_{\psi_e}\frac{\mathrm{c}_\phi}{\mathrm{c}_\theta} + u\frac{\mathrm{s}_{\psi_e}\mathrm{c}_{\psi_e}\mathrm{c}_\theta}{e_d} + v\frac{\mathrm{s}_{\psi_e}\mathrm{c}_{\psi_e}\mathrm{s}_\theta\mathrm{s}_\phi + \mathrm{c}_{\psi_e}^2\mathrm{c}_\phi}{e_d} + w\frac{\mathrm{s}_{\psi_e}\mathrm{c}_{\psi_e}\mathrm{c}_\phi\mathrm{s}_\theta - \mathrm{c}_{\psi_e}^2\mathrm{s}_\phi}{e_d} + \frac{(\dot{x}_d - \delta_x)}{e_d}\left(\mathrm{s}_{\psi_e}\mathrm{c}_{\psi-\psi_e} + \mathrm{s}_\psi\right) + \frac{(\dot{y}_d - \delta_y)}{e_d}\left(\mathrm{s}_{\psi_e}\mathrm{s}_{\psi-\psi_e} - \mathrm{c}_\psi\right). \tag{34}$$

Finally, to solve the robust prescribed performance tracking control problem, we pose the following assumption.

Assumption 2. *The vehicle initializes in such configuration that: a) $e_d(0) > \underline{\rho}_d$, b) $|\psi_e(0)| \leq \bar{\psi}_e < \frac{\pi}{2}$, c) $|\phi(0)| < \bar{\phi} < \frac{\pi}{2}$ and d) $|\theta(0)| < \bar{\theta} < \frac{\pi}{2}$ for an arbitrarily small positive design constant $\underline{\rho}_d$ and some positive constants $\bar{\psi}_e$, $\bar{\phi}$, $\bar{\theta}$ satisfying $\cot\bar{\psi}_e > t_{\bar{\phi}}s_{\bar{\theta}}$.*

Remark 6. *Assumption 2 guarantees via (a) that the orientation error e_o is initially well-defined as well as via (b)-(d) that (32)-(34) are initially controllable with respect to u, w and r. First, notice that $|\psi_e(0)| \leq \bar{\psi}_e < \frac{\pi}{2}$, $|\phi(0)| < \bar{\phi} < \frac{\pi}{2}$ and $|\theta(0)| < \bar{\theta} < \frac{\pi}{2}$ render (34) controllable with respect to r. Additionally, $|\theta(0)| < \bar{\theta} < \frac{\pi}{2}$ guarantees that the vehicle initializes away from the representation singularity (i.e., $\theta = \pm\frac{\pi}{2}$) of the Euler angles' parameterization. Moreover, extracting the input gain matrix [38] of (32) and (33):*

$$G(\phi, \theta, \psi_e) = \begin{bmatrix} -c_{\psi_e}c_\theta & -\left(c_{\psi_e}s_\theta c_\phi + s_{\psi_e}s_\phi\right) \\ s_\theta & -c_\theta c_\phi \end{bmatrix}, \tag{35}$$

considering as inputs the velocities u and w, we can easily derive a sufficient controllability condition (i.e., whether $G(\phi, \theta, \psi_e)$ is invertible) by observing the determinant of $G(\phi, \theta, \psi_e)$:

$$\det\left(G(\phi, \theta, \psi_e)\right) = c_{\psi_e}c_\phi + s_{\psi_e}s_\phi s_\theta,$$

which is initially strictly positive owing to Assumption 2 (i.e., $\cot\left(|\psi_e(0)|\right) \geq \cot\bar{\psi}_e > t_{\bar{\phi}}s_{\bar{\theta}} > t_{|\phi(0)|}s_{|\theta(0)|}$ leads straightforwardly to $\det\left(G\left(\phi(0), \theta(0), \psi_e(0)\right)\right) > c_{\bar{\psi}_e}c_{\bar{\phi}} - s_{\bar{\psi}_e}s_{\bar{\phi}}s_{\bar{\theta}} > 0$). In this respect, we shall design a controller that, besides guaranteeing $e_d(t) > \underline{\rho}_d > 0$, $\forall t \geq 0$, further forces the heading angle ψ_e to satisfy $|\psi_e(t)| \leq \bar{\psi}_e < \frac{\pi}{2}$, $\forall t \geq 0$. Furthermore, since the unactuated roll and pitch degrees of freedom are passive, the corresponding angles will be proven to remain bounded close to the origin satisfying $|\phi(t)| < \bar{\phi}$

and $|\theta(t)| < \bar{\theta}$, $\forall t \geq 0$. Hence, (32)-(34) will remain controllable (i.e., $|\psi_e(t)| \leq \bar{\psi}_e$, $|\phi(t)| < \bar{\phi}$, $|\theta(t)| < \bar{\theta}$ and $\det(G(\phi(t), \theta(t), \psi_e(t))) > 0$, $\forall t \geq 0$) and will evolve away from the representation singularity. Finally, notice from a practical point of view that Assumption 2 can be easily enforced by simply placing the vehicle in an initial configuration that is heading towards the desired trajectory (target), which is quite reasonable in underwater applications.

Control Scheme: Similarly to the torpedo case, the proposed control scheme is first derived at the kinematic level assuming that the control signals are the surge, heave and yaw velocities u, w, r. Subsequently, the kinematic controller is extended to the dynamic model, considering the actual control input signals X, Z, and N (i.e., forces X, Z in surge and heave as well as a torque N in yaw). Hence, given a smooth desired trajectory $\boldsymbol{p}_d(t) = [x_d(t), y_d(t), z_d(t)]^T$ with bounded time derivatives, and any initial vehicle configuration satisfying Assumption 2 for an arbitrarily small positive design constant $\underline{\rho}_d$, the control design proceeds as follows.

Kinematic Controller: *Select position/orientation performance functions $\rho_d(t)$, $\rho_z(t)$, $\rho_o(t)$ that i) satisfy:*

a_{kin}	$e_d(0) < \rho_d(0)$	$\underline{\rho}_d < \rho_d(t)$	$\underline{\rho}_d < \lim_{t\to\infty} \rho_d(t)$
b_{kin}	$\lvert e_z(0)\rvert < \rho_z(0)$	$0 < \rho_z(t)$	$0 < \lim_{t\to\infty} \rho_z(t)$
c_{kin}	$\lvert e_o(0)\rvert < \rho_o(0) \leq \bar{\rho} < 1$	$0 < \rho_o(t)$	$0 < \lim_{t\to\infty} \rho_o(t)$

for a positive constant $\bar{\rho} < 1$ and ii) incorporate the desired performance specifications regarding the steady state error and the speed of convergence (see Subsection I-A2). Subsequently, design the desired velocities:

$$\begin{bmatrix} u_d \\ w_d \end{bmatrix} = -\left[G(\phi,\theta,\psi_e)\right]^{-1} \begin{bmatrix} k_d \ln\left(\dfrac{1+\frac{e_d-\frac{\rho_d(t)+\underline{\rho}_d}{2}}{\frac{\rho_d(t)-\underline{\rho}_d}{2}}}{1-\frac{e_d-\frac{\rho_d(t)+\underline{\rho}_d}{2}}{\frac{\rho_d(t)-\underline{\rho}_d}{2}}}\right) \\ k_z \ln\left(\dfrac{1+\frac{e_z}{\rho_z(t)}}{1-\frac{e_z}{\rho_z(t)}}\right) \end{bmatrix} \tag{36}$$

$$r_d = -k_o \ln\left(\frac{1+\frac{e_o}{\rho_o(t)}}{1-\frac{e_o}{\rho_o(t)}}\right) \tag{37}$$

where $G(\phi,\theta,\psi_e)$ is the input gain matrix defined in (35) and k_d, k_z, k_o are positive control gains.

Dynamic Controller: *Select velocity performance functions $\rho_u(t)$, $\rho_w(t)$, $\rho_r(t)$ that satisfy:*

a_{dyn}	$\lvert u(0) - u_d(0)\rvert < \rho_u(0)$	$0 < \rho_u(t)$	$0 < \lim_{t\to\infty} \rho_u(t)$
b_{dyn}	$\lvert w(0) - w_d(0)\rvert < \rho_w(0)$	$0 < \rho_w(t)$	$0 < \lim_{t\to\infty} \rho_w(t)$
c_{dyn}	$\lvert r(0) - r_d(0)\rvert < \rho_r(0)$	$0 < \rho_r(t)$	$0 < \lim_{t\to\infty} \rho_r(t)$

and design the forces in surge and heave as well as the torque in yaw as:

$$X = -k_u \ln\left(\frac{1+\frac{u-u_d}{\rho_u(t)}}{1-\frac{u-u_d}{\rho_u(t)}}\right) \tag{38}$$

$$Z = -k_w \ln\left(\frac{1+\frac{w-w_d}{\rho_w(t)}}{1-\frac{w-w_d}{\rho_w(t)}}\right) \tag{39}$$

$$N = -k_r \ln\left(\frac{1+\frac{r-r_d}{\rho_r(t)}}{1-\frac{r-r_d}{\rho_r(t)}}\right) \tag{40}$$

with positive control gains k_u, k_w, k_r.

We now summarize the main results of this subsection in the following theorem.

Theorem 3. *Consider any smooth desired trajectory $\boldsymbol{p}_d(t) = [x_d(t), y_d(t), z_d(t)]^T$ with bounded derivatives and a unicycle-like underactuated underwater vehicle modeled by (7), (8) and (9)-(14), in any initial configuration satisfying Assumption 2, for an arbitrarily small positive design constant $\underline{\rho}_d$. The proposed control scheme (36)-(40) guarantees:*

$$\left.\begin{array}{c} \underline{\rho}_d < e_d(t) < \rho_d(t) \\ -\rho_z(t) < e_z(t) < \rho_z(t) \\ -\rho_o(t) < e_o(t) < \rho_o(t) \end{array}\right\}, \forall t \geq 0$$

for appropriately selected performance functions $\rho_d(t)$, $\rho_z(t)$, $\rho_o(t)$ that incorporate the desired transient and steady state performance specifications, and avoids the singularities introduced by the error transformations (30), (31) with bounded closed loop signals, thus leading to the solution of the robust prescribed performance tracking control problem as stated in Subsection II-C.

Proof. *See the Appendix.*

Remark 7. *Initially, based on Assumption 2, the orientation error e_o is well-defined and Eq. (20)-(22) are controllable. Subsequently, the performance functions $\rho_d(t)$ and $\rho_o(t)$ are selected such that the orientation error is retained well defined and the controllability of (20)-(22) is preserved as long as prescribed performance is guaranteed, that is $\underline{\rho}_d < e_d(t) < \rho_d(t)$, $-\rho_o(t) < e_o(t) < \rho_o(t)$, $\forall t \geq 0$. Due to property-c_{kin} (i.e., $\rho_o(t) \leq \bar{\rho} < 1$) the prescribed performance guarantees lead to $e_o^2(t) = s^2_{\psi_e(t)} = 1 - c^2_{\psi_e(t)} \leq \rho_o^2(t) \leq \bar{\rho}^2$ and consequently to $|\psi_e(t)| < \overline{\psi}_e = \cos^{-1}\left(\sqrt{1-\bar{\rho}^2}\right) < \frac{\pi}{2}$, $\forall t \geq 0$. Furthermore, the passivity of the unactuated degrees of freedom (i.e., roll and pitch) ensures that $|\phi(t)| < \bar{\phi}$ and $|\theta(t)| < \bar{\theta}$, $\forall t \geq 0$ for sufficiently small $\bar{\phi}$, $\bar{\theta}$. Therefore, the satisfaction of prescribed performance constitutes a sufficient condition for bypassing the aforementioned singularity issues.*

C. Commentary

1) Control Philosophy: The prescribed performance control technique enforces the normalized position/orientation errors $\xi_d(t) = \frac{e_d - \frac{\rho_d(t)+\underline{\rho}_d}{2}}{\frac{\rho_d(t)-\underline{\rho}_d}{2}}$, $\xi_t(t) = \frac{e_t}{\rho_t(t)}$, $\xi_o(t) = \frac{e_o}{\rho_o(t)}$ $\left(\text{or } \xi_d(t) = \frac{e_d - \frac{\rho_d(t)+\underline{\rho}_d}{2}}{\frac{\rho_d(t)-\underline{\rho}_d}{2}}, \xi_z(t) = \frac{e_z}{\rho_z(t)}, \xi_o(t) = \frac{e_o}{\rho_o(t)}\right)$ and

velocity errors $\xi_u(t) = \frac{e_u}{\rho_u(t)}$, $\xi_q(t) = \frac{e_q}{\rho_q(t)}$, $\xi_r(t) = \frac{e_r}{\rho_r(t)}$ $\left(\text{or } \xi_u(t) = \frac{e_u}{\rho_u(t)}, \xi_w(t) = \frac{e_w}{\rho_w(t)}, \xi_r(t) = \frac{e_r}{\rho_r(t)}\right)$, with $e_u \triangleq u - u_d$, $e_w \triangleq w - w_d$, $e_q \triangleq q - q_d$ and $e_r \triangleq r - r_d$, to remain strictly within the set $(-1, 1)$ for all $t \geq 0$. Notice that modulating $\xi_i(t)$, $i \in \{d, t, o, u, q, r\}$ (or $i \in \{d, z, o, u, w, r\}$) via the logarithmic function $\ln\left(\frac{1+\star}{1-\star}\right)$ in the control signals (23)-(28) (or (36)-(40)) and selecting $\rho_i(0) > |e_i(0)|$, $i \in \{d, t, o, u, q, r\}$ (or $i \in \{d, z, o, u, w, r\}$), the control signals $\varepsilon_i(\xi_i) = \ln\left(\frac{1+\xi_i}{1-\xi_i}\right)$, $i \in \{d, t, o, u, q, r\}$ (or $i \in \{d, z, o, u, w, r\}$) are initially well-defined. Moreover, it is not difficult to verify that maintaining simply the boundedness of the modulated errors $\varepsilon_i(\xi_i(t))$, $i \in \{d, t, o, u, q, r\}$ (or $i \in \{d, z, o, u, w, r\}$) for all $t \geq 0$ is equivalent to guaranteeing $\xi_i(t) \in (-1, 1)$, $i \in \{d, t, o, u, q, r\}$ (or $i \in \{d, z, o, u, w, r\}$) for all $t \geq 0$. Therefore, the problem at hand can be visualized as stabilizing the modulated errors $\varepsilon_i(\xi_i(t))$, $i \in \{d, t, o, u, q, r\}$ (or $i \in \{d, z, o, u, w, r\}$), within the feasible regions defined via $\xi_i \in (-1, 1)$, $i \in \{d, t, o, u, q, r\}$ (or $i \in \{d, z, o, u, w, r\}$) for all $t \geq 0$. A careful inspection of the proposed control scheme (23)-(28) (or (36)-(40)) reveals that it actually operates similarly to barrier functions in constrained optimization, admitting high negative or positive values depending on whether $e_d(t) \to \rho_d(t)$ or $e_d(t) \to \underline{\rho}_d$ and $e_i(t) \to \rho_i(t)$ or $e_i(t) \to -\rho_i(t)$, $i \in \{t, o, u, q, r\}$ (or $i \in \{z, o, u, w, r\}$); eventually preventing $e_i(t)$, $i \in \{d, t, o, u, q, r\}$ (or $i \in \{d, z, o, u, w, r\}$) from reaching the corresponding boundaries.

2) Structural Complexity: The proposed control schemes do not incorporate any prior knowledge of the external disturbances and the vehicle's dynamic model parameters or even of some corresponding upper bounding constants. Furthermore, no estimation (i.e., adaptive control) has been employed to acquire such knowledge. Moreover, compared with the traditional backstepping-like approaches, the proposed schemes prove significantly less complex. Notice that no hard calculations are required to output the proposed control signals, thus making implementation straightforward. Finally, it should be noted that no velocity measurements of the unactuated degrees of freedom (i.e., sway-heave-roll and sway-roll-pitch velocities for the torpedo-like and unicycle-like underactuated vehicles respectively) are incorporated in the control schemes, thus greatly increasing the robustness against noises that corrupt the specific measurements and simplifying further the implementation.

3) Robust Prescribed Performance: It is worth noticing that the proposed control schemes achieve their goals without residing to the need of rendering $\varepsilon_i(t)$, $i \in \{d, t, o, u, q, r\}$ (or $i \in \{d, z, o, u, w, r\}$) arbitrarily small, through extreme values of the control gains k_i, $i \in \{d, t, o, u, q, r\}$ (or $i \in \{d, z, o, u, w, r\}$). More specifically, notice that (51)-(55) and (59) hold no matter how large the finite bounds $\bar{\varepsilon}_i$, $i \in \{d, t, o, u, q, r\}$ and $i \in \{d, z, o, u, w, r\}$ are. In the same spirit, large model uncertainties, either in the vehicle parameters or the external disturbances, can be compensated, as they affect only the size of $\bar{\varepsilon}_i$, $i \in \{d, t, o, u, q, r\}$ and $i \in \{d, z, o, u, w, r\}$, but leave the achieved stability properties unaltered as shown in (51)-(55) and (59). Hence, the actual tracking performance given in Theorem 2 and Theorem 3, which is solely determined by the designer-specified performance functions $\rho_i(t)$, $i \in \{d, t, o\}$ and $i \in \{d, z, o\}$, becomes isolated against model uncertainties, thus greatly extending the robustness of the proposed control schemes.

4) Control Parameters Selection: Unlike what is common practice in the related literature, the performance of the closed loop system is explicitly and solely determined by appropriately selecting the parameter $\underline{\rho}_d$ and the position/orientation performance functions $\rho_i(t)$, $i \in \{d, t, o, \}$ (or $i \in \{d, z, r\}$). In particular, the decreasing rate of $\rho_i(t)$, $i \in \{d, t, o, \}$ (or $i \in \{d, z, r\}$) introduces directly a lower bound on the speed of convergence of the corresponding position/orientation errors. Furthermore, $\underline{\rho}_d$ and $\lim_{t\to\infty} \rho_i(t)$, $i \in \{d, t, o, \}$ (or $i \in \{d, z, r\}$) regulate the maximum allowable size of the position/orientation errors at steady state. In that respect, the performance attributes of the proposed control schemes are selected a priori, in accordance to the desired transient and steady state performance specifications. In this way, the selection of the control gains k_i, $i \in \{d, t, o, u, q, r\}$ (or $i \in \{d, z, o, u, w, r\}$), that has been isolated from the actual control performance, is significantly simplified to adopting those values that lead to reasonable control effort. Nonetheless, it should be noted that their selection affects both the quality of evolution of the position/orientation errors inside the corresponding performance envelopes as well as the control input characteristics (i.e., decreasing the gain values leads to increased oscillatory behaviour within the prescribed performance envelopes, which is improved when adopting higher values, enlarging, however, the control effort both in magnitude and rate). Additionally, fine tuning might be needed in real-time scenarios, to retain the required control input signals within the feasible range that can be implemented by the actuators. Similarly, the control input constraints impose an upper bound on the required speed of convergence of the position/orientation performance functions as well as on the uncertainty level, either from the model or the external disturbances, that can be handled by the proposed control schemes. Hence, the selection of the control gains k_i, $i \in \{d, t, o, u, q, r\}$ (or $i \in \{d, z, o, u, w, r\}$) can have positive influence on the overall closed loop system response. In the same spirit, although performance specifications are not required for the velocity errors, the selection of the corresponding velocity performance functions $\rho_i(t)$, $i \in \{u, q, r\}$ (or $i \in \{u, w, r\}$) affects both the evolution of the position errors within the corresponding performance envelopes as well as the control input characteristics (i.e., relaxing the convergence rate and the steady state limit of the velocity performance functions leads to increased oscillatory behavior, which is improved when considering tighter performance functions, enlarging, however, the control effort both in magnitude and rate). Nevertheless, the only hard constraint attached to their definition is related to their initial values.

5) Minimal Tracking Information: Interestingly, the proposed control schemes are independent of the time derivatives of $\boldsymbol{p}_d(t) = [x_d(t), y_d(t), z_d(t)]^T$. Regarding the torpedo-like (or unicycle-like) underactuated vehicles, the desired

velocities u_d, q_d, r_d (or u_d, w_d, r_d) depend only on $\boldsymbol{p}_d(t) = [x_d(t), y_d(t), z_d(t)]^T$. However, $\dot{u}_d$, $\dot{q}_d$, $\dot{r}_d$ (or $\dot{u}_d$, $\dot{w}_d$, $\dot{r}_d$) which involve $\dot{\boldsymbol{p}}_d(t) = [\dot{x}_d(t), \dot{y}_d(t), \dot{z}_d(t)]^T$, are proven bounded and therefore, we do not compensate for them through the design of the control signals X, M, N (or X, Z, N). Thus, applications where the desired trajectory is not a priori known for all time but it is computed on-line (e.g., tracking a moving target where the desired trajectory - target position - is obtained at each time instant via a measuring device and is unknown before hand) and thus its time derivatives are not available (numerical differentiation typically does not help in this direction since it may introduce large errors), can be successfully and efficiently tackled.

IV. Simulations

To demonstrate the proposed approach and point out its intriguing performance properties with respect to existing results in the related literature, a comparative simulation study with the well-established PID control law was conducted for an underwater pipeline inspection task under external disturbances representing ocean currents and waves. More specifically, we considered the tracking control problem of a multi-sector trajectory along a complex pipeline structure, involving line and curved segments as well as vertical and horizontal helixes, for a torpedo-like underactuated underwater vehicle.

The dynamics of a 6 DoF model (the parameters of the dynamic model were found in [39]) and the motion control scheme was simulated in UWSim [40], a realistic simulation environment developed in the Robot Operating System (ROS) framework, using a 4-th order Runge-Kutta integration method with 1 ms time step. The vehicle initialized at rest from the configuration $x(0) = -38.0$ m, $y(0) = -9.1$ m, $z(0) = 27.8$ m, $R(0) = \mathrm{diag}([-1, -1, 1])$ and was requested to track a multi-sector trajectory along the pipeline with maximum steady state position error 0.3 m and minimum convergence rate as obtained by the exponential $\exp(-0.1t)$. Additionally, we considered that the vehicle's motion was affected by external disturbances representing a constant ocean current of the form $\delta_x(t) = -0.25$ m/s, $\delta_y(t) = 0.25$ m/s, $\delta_z(t) = 0$ m/s (the direction of the ocean stream is depicted in Fig. 5 with green arrows) and harmonic waves modeled by three random sinusoids with amplitude and frequency equally distributed in $[0.1, 1]$ N (for the translational dynamics), $[0.1, 1]$ Nm (for the rotational dynamics) and $[0.01, 0.1]$ rad/s respectively.

Given the initial configuration of the vehicle as well as the required performance specifications and following Subsections III-A and III-C, we selected the performance functions $\rho_d(t) = (6.0 - 0.3)\exp(-0.1t) + 0.3$, $\rho_t(t) = (0.6 - 0.1)\exp(-t) + 0.1$, $\rho_o(t) = (0.6 - 0.1)\exp(-t) + 0.1$, $\rho_u(t) = (2 - 0.1)\exp(-1.5t) + 0.1$, $\rho_q(t) = (2 - 0.1)\exp(-1.5t) + 0.1$, $\rho_r(t) = (2 - 0.1)\exp(-1.5t) + 0.1$ and the control gains $k_d = 10$, $k_o = 2$, $k_t = 2$, $k_u = 100$, $k_q = 20$, $k_r = 20$ such that (23)-(28) yield reasonable control effort. Furthermore, it should be noticed that Assumption 1 is satisfied by the aforementioned initial configuration for $\underline{\rho}_d = 0.1$. Finally, a fair comparison with the PID controller

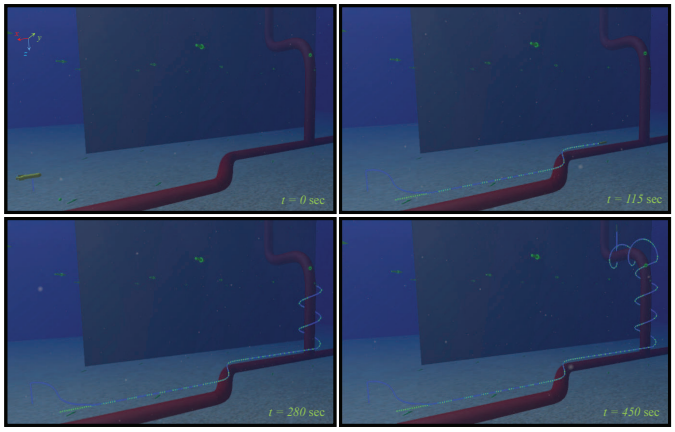

Fig. 5: Simulation: The trace of the vehicle (blue line) along with the desired trajectory (green line).

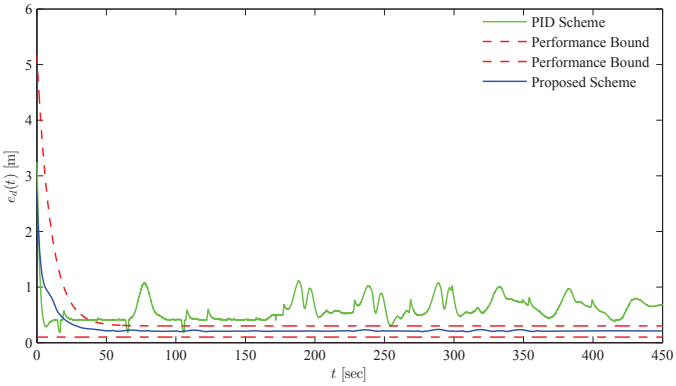

Fig. 6: Simulation: The tracking error evolution. The red dashed lines indicate the desired performance bounds. The blue and green solid lines indicate the evolution of $e_d(t)$ for the proposed and the PID control schemes respectively.

was achieved by setting appropriately its gains, following the pole placement method, in order to achieve the desired performance specifications, based on a realistic case, where the model parameters, that were adopted in the approximate linearization technique, deviated up to 10% from their actual values.

The trajectory tracking of the proposed scheme is shown in Fig. 5 for 4 consecutive time instants. The distance error of both the proposed scheme and the PID controller along with the desired performance bounds are pictured in Fig. 6. The evolution of the orientation errors under the proposed control law along with the corresponding performance bounds is depicted in Fig. 7. Finally, the body velocities and the requested control effort under the proposed scheme are given in Figs. 8 and 9 respectively. Notice that as it was predicted by the theoretical analysis, tracking with prescribed performance and bounded control signals is achieved despite the presence of external disturbances and the lack of knowledge of the vehicle's dynamic model parameters. On the contrary, although the response of the PID controller, as observed in Fig. 6, was quite satisfactory during the transient and along the line segments of the desired trajectory, where the linearization is rather accurate, it should be noted that the error increased up to almost 1.5 m with a quite unsatisfactory response during the helical segments, where the linearization was not adequate, owing to the large operating envelope and the system uncertainty. In this way, it is verified that the proposed

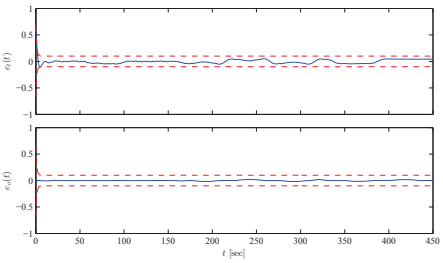

Fig. 7: Simulation: The orientation tracking error evolution. The red dashed lines indicate the desired performance bounds. The blue solid lines indicate the evolution of $e_t(t)$ and $e_o(t)$.

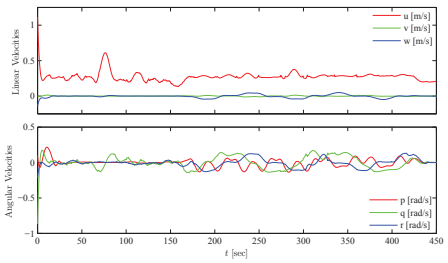

Fig. 8: Simulation: The linear and angular velocities.

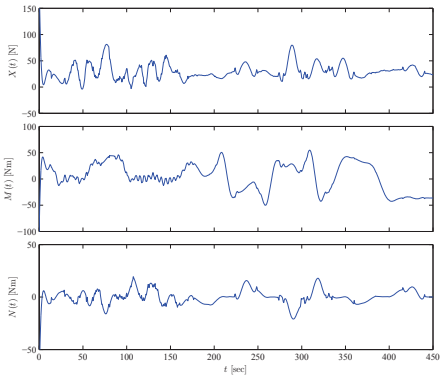

Fig. 9: Simulation: The control commands in surge (X), pitch (M) and yaw (N).

scheme outperforms the well-established PID controller in challenging operating conditions, that are commonly met in underwater applications. An accompanying video demonstrating the aforementioned simulation study may be found in https://youtu.be/2cNN3ksPjd4.

V. Experiment

To verify the tracking performance and robustness of the proposed scheme, an experimental procedure was carried out inside a water tank using a small remotely operated underwater vehicle. The deployed vehicle VideoRay PRO is equipped with three thrusters, affecting surge-heave-yaw motions (i.e., it falls within the class of unicycle-like underactuated vehicles) and its control unit is connected with a host computer through a serial communication interface (RS-232). Additionally, a Polhemus-Isotrack device, interfaced to the host computer via RS-232 serial communication at 30 Hz, was employed as a pose feedback sensor for the motion control scheme. The Isotrak tracking system consists of a transmitter and a receiver (tracker) and uses electro-magnetic fields to determine the tracker's position/orientation. In our case, the transmitter was placed at a fixed spot outside the water tank and the tracker was mounted on the vehicle. Finally, the overall software architecture was developed in C++ on a Linux operating system.

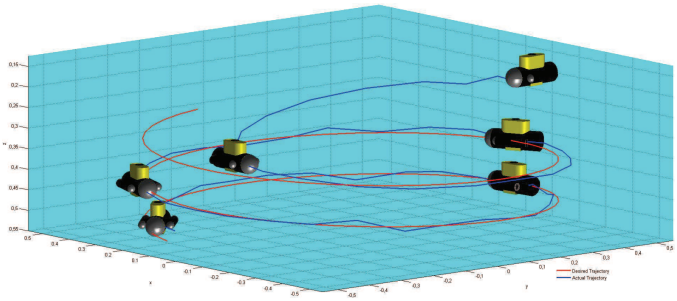

Fig. 10: Experiment: The trace of the vehicle (blue line) along with the desired trajectory (red line).

The vehicle initialized at rest from the configuration $x(0) = 0.22$ m, $y(0) = 0.76$ m, $z(0) = 0.27$ m, $\phi(0) = 0.1°$, $\theta(0) = 1.2°$ and $\psi(0) = -94.59°$ and was requested to track a helical trajectory towards the bottom of the tank described by $x_d(t) = 0.4\cos(0.1\pi t)$ m, $y_d(t) = -0.4\sin(0.1\pi t)$ m, $z_d(t) = 0.3 + 0.015t$ m, with maximum steady state error 0.2 m and minimum convergence rate as obtained by the exponential $\exp(-0.25t)$. Notice that the aforementioned initial configuration satisfied Assumption 2 for $\underline{\rho}_d = 0.05$. Hence, following Subsection III-B, we selected the performance functions:

$$\begin{aligned}
\rho_d(t) &= (2.0 - 0.15)\exp(-0.25t) + 0.15\\
\rho_z(t) &= (0.5 - 0.05)\exp(-0.25t) + 0.05\\
\rho_o(t) &= (0.8 - 0.08)\exp(-0.25t) + 0.08\\
\rho_u(t) &= (2 - 0.5)\exp(-0.25t) + 0.5\\
\rho_w(t) &= (2 - 0.5)\exp(-0.25t) + 0.5\\
\rho_r(t) &= (2 - 0.5)\exp(-0.25t) + 0.5
\end{aligned}$$

and the control gains $k_d = 0.3$, $k_z = 1$, $k_o = 1$, $k_u = 7.5$, $k_w = 5.0$, $k_r = 0.25$ such that (36)-(40) yield reasonable control effort.

The trace of the vehicle along with the desired trajectory is illustrated in Fig. 10. As it was predicted by the theoretical analysis and is actually depicted in Figs. 11 and 12, stable tracking with prescribed performance is successfully achieved, with the errors evolving strictly within the predefined performance bounds, despite the lack of knowledge regarding the vehicle's dynamic model parameters. Additionally, as it is pictured in Fig. 13 the required control effort was satisfactorily smooth and did not impose any saturation to the thrusters (the limits of the considered vehicle for the X, Z and N degrees of actuation are 15 N, 7.5 N and 1 Nm respectively).

The existing setup did not allow us to create external disturbances in the form of waves and currents. However, the power & communication tether attached to the vehicle, was creating non-trivial external disturbances in the form of random forces and torques, as the vehicle was constantly changing configuration during the experiment. As it can be seen from Fig. 11 and the overall performance of the controller, the aforementioned external disturbances were rejected successfully, thus verifying the efficiency and robustness of the proposed control scheme. The aforementioned experimental study is demonstrated in the accompanying video.

VI. Conclusions

This paper proposed a solution for the 3D trajectory tracking control problem for torpedo-like and unicycle-like underactuated underwater vehicles. The derived control schemes guarantee tracking with prescribed transient and steady state performance despite the presence of external disturbances and without requiring prior information of the vehicle's model

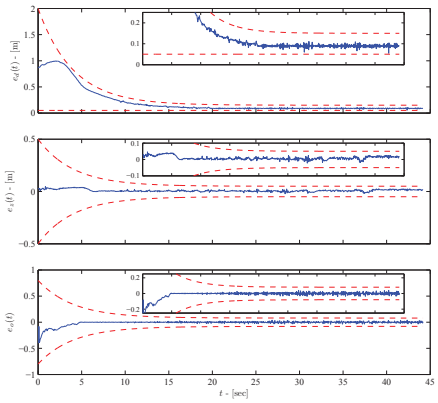

Fig. 11: Experiment: The tracking error evolution. The red dashed lines indicate the desired performance bounds. The blue solid lines indicate the evolution of $e_d(t)$, $e_z(t)$ and $e_o(t)$. The subplots give details at the steady state.

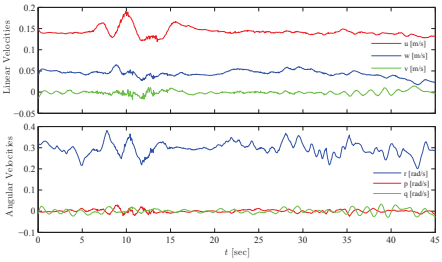

Fig. 12: Experiment: The linear and angular velocities.

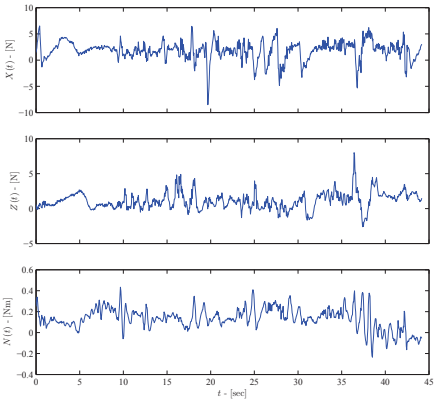

Fig. 13: Experiment: The control commands in surge (X), heave (Z) and yaw (N).

parameters. Moreover, no velocity measurement of the unactuated degrees of freedom is needed, thus increasing its robustness against noises that corrupt the corresponding measurements. Furthermore, only the desired trajectory and none of its higher order derivatives is incorporated in the control scheme. Additionally, the proposed control schemes are of low complexity and avoid both controllability and representation singularities that appear inherently during the control design procedure. Finally, simulation and experimental results clarified and verified the proposed approach.

Future research directions will be devoted towards studying the effect of: i) **input uncertainties** (i.e., mapping uncertainties between desired body forces/torques and actuator commands) and **constraints** (e.g., the thruster limitations as well as in case of torpedo-like vehicles with stern fins, the coupling of pitch and yaw control input torques with the surge velocity via (15)) as well as ii) **sensor filtering** (underwater localization is mainly based on acoustic sensors, which however are plagued with noise, intermittent failures and latency) on the closed loop stability, in order to increase the applicability of the proposed control methodologies in open sea scenarios. Extra attention should also be devoted on studying how the achieved transient and steady state performance specifications could encapsulate further configuration constraints that may arise owing to the limited capabilities of on board sensors (e.g., the limited field of view of cameras or sonars) that may be adopted to track the desired target. Such a property would be quite significant especially in high-demanding inspection and surveillance tasks, where the target must always be kept inside the sensor's field of view. Moreover, introducing the Cartesian error representation instead of the spherical/polar that is adopted in this work might lead to simpler error dynamics and avoid singularities, thus yielding even more reduced design complexity. Finally, the increasingly challenging mission scenarios in the field of marine robotics, ranging from exploration and surveillance to seabed mapping and reconnaissance call for inexpensive and robust control solutions. Thus, the extension of the intrinsic properties of the proposed methodologies to a fleet of multiple cooperating underwater vehicles should also be addressed.

APPENDIX

Proof of Theorem 2

Let us define the normalized errors:

$$\xi_d = \frac{e_d - \frac{\rho_d(t)+\underline{\rho}_d}{2}}{\frac{\rho_d(t)-\underline{\rho}_d}{2}},\ \xi_t = \frac{e_t}{\rho_t(t)},\ \xi_o = \frac{e_o}{\rho_o(t)}, \tag{41}$$

$$\xi_u = \frac{u-u_d}{\rho_u(t)},\ \xi_q = \frac{q-q_d}{\rho_q(t)},\ \xi_r = \frac{r-r_d}{\rho_r(t)}. \tag{42}$$

In this respect, the desired velocities (23)-(25) and the control law (26)-(28) may be written as functions of the normalized errors ξ_i, $i \in \{d,t,o,u,q,r\}$ as follows:

$$u_d = k_d \ln\left(\frac{1+\xi_d}{1-\xi_d}\right),\ q_d = -k_t \ln\left(\frac{1+\xi_t}{1-\xi_t}\right),\ r_d = k_o \ln\left(\frac{1+\xi_o}{1-\xi_o}\right), \tag{43}$$

$$X = -k_u \ln\left(\frac{1+\xi_u}{1-\xi_u}\right),\ M = -k_q \ln\left(\frac{1+\xi_q}{1-\xi_q}\right),\ N = -k_r \ln\left(\frac{1+\xi_r}{1-\xi_r}\right). \tag{44}$$

Let us now define the overall state vector:

$$\boldsymbol{\xi} = \left[\xi_d, \xi_o, \xi_t, \xi_u, \xi_q, \xi_r, \boldsymbol{s}^T\right]^T,$$

where $\boldsymbol{s} = [v, w, p]^T$ denotes the unactuated velocities (i.e., sway, heave and roll velocities). Differentiating the normalized errors (41), (42) with respect to time and substituting (9)-(14), (20)-(22) as well as (43), (44), we obtain in a compact form, the closed loop dynamical system:

$$\dot{\boldsymbol{\xi}} = h\left(t, \boldsymbol{\xi}\right) \tag{45}$$

where the function $h\left(t, \boldsymbol{\xi}\right)$ includes all terms found in the right hand side[5], after the differentiation of $\boldsymbol{\xi}$. Let us also define the set $\Omega_{\boldsymbol{\xi}} = \underbrace{(-1,1) \times \cdots \times (-1,1)}_{\text{6-times}} \times \Omega_{\boldsymbol{s}}$, where $\Omega_{\boldsymbol{s}} = \left\{\boldsymbol{s} \in \Re^3 : \|\boldsymbol{s}\| < \bar{s}\right\}$ is an open set with $\bar{s}$ denoting a positive constant to be specified later, for analysis purposes only.

[5]Notice that the time argument of $h\left(t, \boldsymbol{\xi}\right)$ encapsulates implicitly the effect of the desired trajectory $\boldsymbol{p}_d\left(t\right)$, the performance functions $\rho_i\left(t\right)$, $i \in \{d,o,t,u,q,r\}$ and the external disturbance terms $\delta_{\mathbf{c}}\left(t\right)$ and $\delta_i\left(t\right)$, $i \in \{u,v,w,p,q,r\}$ on the closed loop system dynamics.

In the sequel, we proceed in two phases. First, the existence and uniqueness of a maximal solution $\boldsymbol{\xi}(t)$ of (45) over the set $\Omega_{\boldsymbol{\xi}}$ for a time interval $[0, \tau_{\max})$ is ensured (i.e., $\boldsymbol{\xi}(t) \in \Omega_{\boldsymbol{\xi}}$, $\forall t \in [0, \tau_{\max})$). Then, we prove that the proposed control scheme guarantees, for all $t \in [0, \tau_{\max})$: a) the boundedness of all closed loop signals of (45) as well as that b) $\boldsymbol{\xi}(t)$ remains strictly within a compact subset of $\Omega_{\boldsymbol{\xi}}$, which subsequently will lead to $\tau_{\max} = \infty$ by contradiction and consequently to the solution of the tracking control problem stated in Subsection II-C. Moreover, notice that the design parameter $\underline{\rho}_d$ and the performance functions $\rho_d(t)$, $\rho_t(t)$, $\rho_o(t)$ were selected (see Subsection III-A) such that no singular point lies in $\Omega_{\boldsymbol{\xi}}$ (i.e., $e_d > \underline{\rho}_d > 0$ and $|\theta_n| \leq \bar{\theta}_n < \frac{\pi}{2}$, $\forall \boldsymbol{\xi} \in \Omega_{\boldsymbol{\xi}}$). In this respect, the proposed scheme avoids the singularity issues mentioned in Subsection III-A, which have been the main drawbacks in similar control approaches for underactuated underwater vehicles, via guaranteeing that $\boldsymbol{\xi}(t)$ remains strictly within a compact subset of $\Omega_{\boldsymbol{\xi}}$.

Phase A. The set $\Omega_{\boldsymbol{\xi}}$ is nonempty and open. Moreover, owing to the selection of the performance functions $\rho_i(t)$, $i \in \{d, t, o, u, q, r\}$ as well as to Assumption 1, we conclude that $\boldsymbol{\xi}(0) \in \Omega_{\boldsymbol{\xi}}$ for a positive constant $\bar{s}$ satisfying $\|\boldsymbol{s}(0)\| < \bar{s}$. Additionally, due to the smoothness of: a) the system nonlinearities, b) the desired trajectory and c) the proposed control scheme over $\Omega_{\boldsymbol{\xi}}$, it can be easily verified that $h(t, \boldsymbol{\xi})$ is continuous on t and continuous for all $\boldsymbol{\xi} \in \Omega_{\boldsymbol{\xi}}$. Therefore, the hypotheses of Theorem 1 stated in Subsection I-A3 hold and the existence and uniqueness of a maximal solution $\boldsymbol{\xi}(t)$ of (45) on a time interval $[0, \tau_{\max})$ such that $\boldsymbol{\xi}(t) \in \Omega_{\boldsymbol{\xi}}$, $\forall t \in [0, \tau_{\max})$ is ensured.

Phase B. We have proven in Phase A that $\boldsymbol{\xi}(t) \in \Omega_{\boldsymbol{\xi}}$, $\forall t \in [0, \tau_{\max})$ or equivalently that:

$$\xi_i(t) \in (-1, 1), \; i \in \{d, t, o, u, q, r\} \tag{46}$$

and $|\boldsymbol{s}(t)| < \bar{s}$ for all $t \in [0, \tau_{\max})$. Therefore, the signals:

$$\varepsilon_i(t) = \ln\left(\frac{1+\xi_i(t)}{1-\xi_i(t)}\right), \; i \in \{d, t, o, u, q, r\} \tag{47}$$

are well defined for all $t \in [0, \tau_{\max})$. Consider now the positive definite and radially unbounded function $V_d = \frac{1}{2}\varepsilon_d^2$. Differentiating with respect to time and substituting (20), we obtain:

$$\dot{V}_d = \frac{4\varepsilon_d}{\left(1-\xi_d^2\right)\left(\rho_d(t)-\underline{\rho}_d\right)}\Big(-u\mathrm{c}_{\theta_n} - v\mathrm{c}_{\theta_o} - w\mathrm{c}_{\theta_t} + \frac{e_x(\dot{x}_d-\delta_x)+e_y\left(\dot{y}_d-\delta_y\right)+e_z(\dot{z}_d-\delta_z)}{e_d} - \frac{(1+\xi_d)\dot{\rho}_d(t)}{2}\Big). \tag{48}$$

Incorporating $u = u_d + \xi_u \rho_u(t)$ from (42) and substituting u_d from (43) and ε_d from (47), $\dot{V}_d$ becomes:

$$\dot{V}_d = \frac{4\varepsilon_d}{\left(1-\xi_d^2\right)\left(\rho_d(t)-\underline{\rho}_d\right)}\Big(-\xi_u\rho_u(t)\,\mathrm{c}_{\theta_n} - v\mathrm{c}_{\theta_o} - w\mathrm{c}_{\theta_t} + \frac{e_x(\dot{x}_d-\delta_x)+e_y\left(\dot{y}_d-\delta_y\right)+e_z(\dot{z}_d-\delta_z)}{e_d} - \frac{(1+\xi_d)\dot{\rho}_d(t)}{2} - k_d\varepsilon_d\mathrm{c}_{\theta_n}\Big).$$

Furthermore, utilizing: i) (46), ii) the fact that $\dot{\rho}_d(t)$, $\rho_u(t)$, $\dot{x}_d(t)$, $\dot{y}_d(t)$, $\dot{z}_d(t)$, $\delta_x(t)$, $\delta_y(t)$, $\delta_z(t)$ are bounded by construction and by assumption and iii) $\|\boldsymbol{s}(t)\| < \bar{s}$, we arrive at:

$$\begin{aligned}&\Big|-\xi_u\rho_u(t)\,\mathrm{c}_{\theta_n} - v\mathrm{c}_{\theta_o} - w\mathrm{c}_{\theta_t} + \frac{e_x(\dot{x}_d-\delta_x)+e_y\left(\dot{y}_d-\delta_y\right)+e_z(\dot{z}_d-\delta_z)}{e_d} - \frac{(1+\xi_d)\dot{\rho}_d(t)}{2}\Big| \\ &\leq \rho_u(0) + \bar{s} + \sup_{t\geq 0}\left\{\left\| \begin{array}{c} \dot{x}_d(t)-\delta_x(t) \\ \dot{y}_d(t)-\delta_y(t) \\ \dot{z}_d(t)-\delta_z(t) \end{array}\right\| + |\dot{\rho}_d(t)|\right\} := \bar{F}_d,\end{aligned} \tag{49}$$

for an unknown positive constant $\bar{F}_d$. Moreover, $\frac{1}{\left(1-\xi_d^2\right)} > 1$ and as mentioned earlier $\mathrm{c}_{\theta_n} \geq \mathrm{c}_{\bar{\theta}_n} > 0$ and $\rho_d(t) - \underline{\rho}_d > 0$. Therefore, we conclude that $\dot{V}_d$ is negative when $|\varepsilon_d(t)| > \frac{\bar{F}_d}{k_d \mathrm{c}_{\bar{\theta}_n}}$ and consequently that:

$$|\varepsilon_d(t)| \leq \bar{\varepsilon}_d = \max\left\{|\varepsilon_d(0)|, \frac{\bar{F}_d}{k_d\mathrm{c}_{\bar{\theta}_n}}\right\}, \tag{50}$$

for all $t \in [0, \tau_{\max})$, which from (47), by applying the inverse logarithmic function, leads to:

$$-1 < \frac{\exp(-\bar{\varepsilon}_d)-1}{\exp(-\bar{\varepsilon}_d)+1} = \underline{\xi_d} \leq \xi_d(t) \leq \overline{\xi_d} = \frac{\exp(\bar{\varepsilon}_d)-1}{\exp(\bar{\varepsilon}_d)+1} < 1 \tag{51}$$

for all $t \in [0, \tau_{\max})$. Hence, the desired velocity u_d also remains bounded (i.e., $|u_d(t)| \leq k_d\bar{\varepsilon}_d$) for all $t \in [0, \tau_{\max})$. Furthermore, following similar analysis for (21) and (22) with the positive definite and radially unbounded functions $V_t = \frac{1}{2}\varepsilon_t^2$, $V_o = \frac{1}{2}\varepsilon_o^2$, we arrive at $|\varepsilon_t(t)| \leq \bar{\varepsilon}_t = \max\left\{|\varepsilon_t(0)|, \frac{\bar{F}_t}{k_t\mathrm{c}_{\bar{\theta}_n}}\right\}$, $|\varepsilon_o(t)| \leq \bar{\varepsilon}_o = \max\left\{|\varepsilon_o(0)|, \frac{\bar{F}_o}{k_o\mathrm{c}_{\bar{\theta}_n}}\right\}$, $\forall t \in [0, \tau_{\max})$ for some positive constants $\bar{F}_o$, $\bar{F}_t$ satisfying similar inequalities to (49), which further lead to:

$$-1 < \frac{\exp(-\bar{\varepsilon}_d)-1}{\exp(-\bar{\varepsilon}_d)+1} = \underline{\xi_t} \leq \xi_t(t) \leq \overline{\xi_t} = \frac{\exp(\bar{\varepsilon}_d)-1}{\exp(\bar{\varepsilon}_d)+1} < 1 \tag{52}$$

$$-1 < \frac{\exp(-\bar{\varepsilon}_d)-1}{\exp(-\bar{\varepsilon}_d)+1} = \underline{\xi_o} \leq \xi_o(t) \leq \overline{\xi_o} = \frac{\exp(\bar{\varepsilon}_d)-1}{\exp(\bar{\varepsilon}_d)+1} < 1. \tag{53}$$

Moreover, the desired velocities q_d, r_d remain bounded as well (i.e., $|q_d(t)| \leq k_t\bar{\varepsilon}_t$, $|r_d(t)| \leq k_o\bar{\varepsilon}_o$, $\forall t \in [0, \tau_{\max})$). Thus, invoking (42), it is straightforward to deduce the boundedness of $u(t)$, $q(t)$, $r(t)$ (i.e., $|u(t)| \leq \bar{u} := \rho_u(0) + k_d\bar{\varepsilon}_d$, $|q(t)| \leq \bar{q} := \rho_q(0) + k_t\bar{\varepsilon}_t$, $|r(t)| \leq \bar{r} := \rho_r(0) + k_o\bar{\varepsilon}_o$, $\forall t \in [0, \tau_{\max})$) and consequently, by differentiating (43) with respect to time and after some straightforward algebraic manipulations, the boundedness of $\dot{u}_d(t)$, $\dot{q}_d(t)$, $\dot{r}_d(t)$, $\forall t \in [0, \tau_{\max})$.

Applying the aforementioned line of proof for the dynamics of the velocity errors ε_u, ε_q, ε_r defined in (47), that involve the dynamic model of the vehicle (9)-(14), considering $V_u = \frac{1}{2}m_u\varepsilon_u^2$, $V_q = \frac{1}{2}m_q\varepsilon_q^2$, $V_r = \frac{1}{2}m_r\varepsilon_r^2$ and the proposed control law (26)-(28), we conclude that:

$$|\varepsilon_i(t)| \leq \bar{\varepsilon}_i = \max\left\{|\varepsilon_i(0)|, \frac{\bar{F}_i}{k_i}\right\}, \; \forall t \in [0, \tau_{\max}) \tag{54}$$

for some positive constants $\bar{F}_i$, $i \in \{u, q, r\}$ that satisfy similar inequalities to (49) relating the performance specifications, the unknown parameters of the dynamic model and the external wave disturbances. Accordingly, we arrive at:

$$-1 < \frac{\exp(-\bar{\varepsilon}_i)-1}{\exp(-\bar{\varepsilon}_i)+1} = \underline{\xi_i} \leq \xi_i(t) \leq \overline{\xi_i} = \frac{\exp(\bar{\varepsilon}_i)-1}{\exp(\bar{\varepsilon}_i)+1} < 1 \tag{55}$$

for all $t \in [0, \tau_{\max})$ and $i \in \{u, q, r\}$, as well as at the boundedness of the control law (26)-(28) for all $t \in [0, \tau_{\max})$ (i.e., $|X(t)| \leq k_u \bar{\varepsilon}_u$, $|M(t)| \leq k_q \bar{\varepsilon}_q$, $|N(t)| \leq k_r \bar{\varepsilon}_r$).

In the sequel, special attention will be paid on the stability of the unactuated velocity vector $\boldsymbol{s} = [v, w, p]^T$. In this way, let us define the positive definite and radially unbounded function $V_{vwp} = \frac{1}{2}\boldsymbol{s}^T \mathrm{diag}([m_v, m_w, m_p])\boldsymbol{s}$ where m_v, m_w, m_p denote the vehicle's mass/moment of inertia and added mass/moment of inertia of the corresponding degrees of freedom. Differentiating V_{vwp} with respect to time and substituting (10)-(12), we obtain:

$$\dot{V}_{vwp} = \boldsymbol{s}^T \mathrm{diag}(\left[Y_v + Y_{|v|v}|v|, Z_w + Z_{|w|w}|w|, K_p + K_{|p|p}|p|\right])\boldsymbol{s} + \boldsymbol{s}^T \begin{bmatrix} -m_u ur + \delta_v(t) \\ m_u uq + \delta_w(t) \\ m_{qr} qr + z_B W \mathrm{c}_\theta \mathrm{s}_\phi + \delta_p(t) \end{bmatrix},$$

which, after straightforward algebraic manipulations, leads to:

$$\dot{V}_{vwp} \leq -\tfrac{\alpha}{\sqrt{3}}\|\boldsymbol{s}\|^3 - \beta\|\boldsymbol{s}\|^2 + F_{vwp}\|\boldsymbol{s}\|,$$

where $\alpha \triangleq \min\left\{\left|Y_{|v|v}\right|, \left|Z_{|w|w}\right|, \left|K_{|p|p}\right|\right\}$, $\beta \triangleq \min\{|Y_v|, |Z_w|, |K_p|\}$ and

$$F_{vwp} := \left\| \begin{array}{c} m_u \bar{u}\bar{r} + \sup_{t\geq 0}\{|\delta_v(t)|\} \\ m_u \bar{u}\bar{q} + \sup_{t\geq 0}\{|\delta_w(t)|\} \\ m_{qr}\bar{q}\bar{r} + |z_B| W + \sup_{t\geq 0}\{|\delta_p(t)|\} \end{array} \right\| \geq \left\| \begin{array}{c} -m_u ur + \delta_v(t) \\ m_u uq + \delta_w(t) \\ m_{qr} qr + z_B W \mathrm{c}_\theta \mathrm{s}_\phi + \delta_p(t) \end{array} \right\|.$$

Therefore, we conclude that $\dot{V}_{vwp}$ is negative when

$$\|\boldsymbol{s}\| > \boldsymbol{S} := \sqrt{\left(\tfrac{\sqrt{3}\beta}{2\alpha}\right)^2 + \tfrac{\sqrt{3}F_{vwp}}{\alpha}} - \tfrac{\sqrt{3}\beta}{2\alpha}$$

and consequently that $\boldsymbol{s}(t) \in \Omega_{\boldsymbol{s}}^{'}$, $\forall t \in [0, \tau_{\max})$, where:

$$\Omega_{\boldsymbol{s}}^{'} = \left\{\boldsymbol{s} \in \Re^3 : \|\boldsymbol{s}\| \leq \bar{\boldsymbol{s}}^{'} := \max\left\{\|\boldsymbol{s}(0)\|, \tfrac{S}{\min\{m_v, m_w, m_p\}}\right\}\right\} \quad (56)$$

is a compact set the size of which depends on: i) the control gain values k_d, k_t, k_o, ii) the control parameters $\rho_u(0)$, $\rho_q(0)$, $\rho_r(0)$, iii) the parameters of the dynamic model (9)-(14), iv) the magnitude of the external disturbances as well as v) implicitly on the desired trajectory and the transient performance specifications.

Up to this point, what remains to be shown is that $t_{\max} = \infty$. Notice that (51)-(53), (55) and (56) imply that $\boldsymbol{\xi}(t) \in \Omega_{\boldsymbol{\xi}}^{'}$, $\forall t \in [0, \tau_{\max})$, where:

$$\Omega_{\boldsymbol{\xi}}^{'} = \prod_{i\in\{d,t,o,u,q,r\}} \left[\tfrac{\exp(-\bar{\varepsilon}_i)-1}{\exp(-\bar{\varepsilon}_i)+1}, \tfrac{\exp(\bar{\varepsilon}_i)-1}{\exp(\bar{\varepsilon}_i)+1}\right] \times \Omega_{\boldsymbol{s}}^{'}$$

is a nonempty and compact set. Moreover, it can be easily verified that $\Omega_{\boldsymbol{\xi}}^{'} \subset \Omega_{\boldsymbol{\xi}}$ for certain, sufficient small[6] control gain values k_d, k_t, k_o and parameters $\rho_u(0)$, $\rho_q(0)$, $\rho_r(0)$ satisfying $\bar{\boldsymbol{s}}^{'} < \bar{\boldsymbol{s}}$. Hence, assuming $\tau_{\max} < \infty$ and since $\Omega_{\boldsymbol{\xi}}^{'} \subset \Omega_{\boldsymbol{\xi}}$, Proposition 1 in Subsection I-A3 dictates the existence of a time instant $t^{'} \in [0, \tau_{\max})$ such that $\boldsymbol{\xi}\left(t^{'}\right) \notin \Omega_{\boldsymbol{\xi}}^{'}$, which is a clear contradiction. Therefore, $\tau_{\max} = \infty$. As a result, all closed loop signals remain bounded and moreover $\boldsymbol{\xi}(t) \in \Omega_{\boldsymbol{\xi}}^{'} \subset \Omega_{\boldsymbol{\xi}}$, $\forall t \geq 0$. Finally, from (41) and (51)-(53), we conclude that:

$$\begin{aligned} \underline{\rho}_d < \tfrac{\exp(-\bar{\varepsilon}_d)-1}{\exp(-\bar{\varepsilon}_d)+1}\tfrac{\rho_d(t)-\underline{\rho}_d}{2} + \tfrac{\rho_d(t)+\underline{\rho}_d}{2} \\ \leq e_d(t) \leq \\ \tfrac{\exp(\bar{\varepsilon}_d)-1}{\exp(\bar{\varepsilon}_d)+1}\tfrac{\rho_d(t)-\underline{\rho}_d}{2} + \tfrac{\rho_d(t)+\underline{\rho}_d}{2} < \rho_d(t) \\ -\rho_t(t) < \tfrac{\exp(-\bar{\varepsilon}_t)-1}{\exp(-\bar{\varepsilon}_t)+1}\rho_t(t) \leq e_t(t) \leq \tfrac{\exp(\bar{\varepsilon}_t)-1}{\exp(\bar{\varepsilon}_t)+1}\rho_t(t) < \rho_t(t) \\ -\rho_o(t) < \tfrac{\exp(\bar{\varepsilon}_o)-1}{\exp(\bar{\varepsilon}_o)+1}\rho_o(t) \leq e_o(t) \leq \tfrac{\exp(\bar{\varepsilon}_o)-1}{\exp(\bar{\varepsilon}_o)+1}\rho_o(t) < \rho_o(t) \end{aligned}$$

for all $t \geq 0$ and consequently the solution of the robust prescribed performance tracking control problem as stated in Subsection II-C, which completes the proof.

Proof of Theorem 3

The proof of this theorem proceeds similarly to Theorem 2. First, we define the normalized errors:

$$\begin{aligned} \xi_d = \frac{e_d - \frac{\rho_d(t)+\underline{\rho}_d}{2}}{\frac{\rho_d(t)-\underline{\rho}_d}{2}},\ \xi_z = \tfrac{e_z}{\rho_z(t)},\ \xi_o = \tfrac{e_o}{\rho_o(t)}, \\ \xi_u = \tfrac{u-u_d}{\rho_u(t)},\ \xi_w = \tfrac{w-w_d}{\rho_w(t)},\ \xi_r = \tfrac{r-r_d}{\rho_r(t)}, \end{aligned} \quad (57)$$

as well as the overall state vector:

$$\boldsymbol{\xi} = \left[\xi_d, \xi_z, \xi_o, \xi_u, \xi_w, \xi_r, \boldsymbol{s}^T\right]^T,$$

where $\boldsymbol{s} = [v, \phi, p, \theta, q]^T$ denotes the state of the unactuated degrees of freedom (i.e., sway, roll and pitch). Differentiating the normalized errors in (57) with respect to time and substituting (9)-(14), (32)-(34) as well as the control scheme (36)-(40), we obtain in a compact form, the closed loop dynamical system:

$$\dot{\boldsymbol{\xi}} = h(t, \boldsymbol{\xi}) \quad (58)$$

where the function $h(t, \boldsymbol{\xi})$ includes all terms found in the right hand side after the differentiation of $\boldsymbol{\xi}$. Let us also define the open set $\Omega_{\boldsymbol{\xi}} = \underbrace{(-1,1) \times \cdots \times (-1,1)}_{\text{6-times}} \times \Omega_{\boldsymbol{s}}$, where $\Omega_{\boldsymbol{s}} = \left\{\boldsymbol{s} \in \Re^5 : \|\boldsymbol{s}\| < \bar{\boldsymbol{s}}\right\}$ is an open set with $\bar{\boldsymbol{s}}$ denoting a positive constant to be specified later for analysis purposes only.

Following the line of proof of Theorem 2 for the signals $\varepsilon_i(t) = \ln\left(\frac{1+\xi_i(t)}{1-\xi_i(t)}\right)$, $i \in \{d, z, o, u, w, r\}$, we conclude for all time $t \in [0, \tau_{\max})$ of the maximal solution $\boldsymbol{\xi}(t)$ of the closed loop system (58) that:

$$|\varepsilon_i(t)| \leq \bar{\varepsilon}_i := \max\left\{|\varepsilon_i(0)|, \bar{F}_i\right\}, i \in \{d, z, o, u, w, r\},$$

where $\bar{F}_i$, $i \in \{d, z, o, u, w, r\}$ denote unknown positive constants that depend on the control gains, the desired trajectory, the performance specifications, the unknown parameters of the dynamic model and the external disturbances. Subsequently, we deduce the boundedness of $u(t)$, $w(t)$, $r(t)$ (i.e.,

[6]Depending on the transient performance specifications, the values of the parameters of the dynamic model and the magnitude of the external disturbances.

$|u(t)| \leq \bar{u} := \rho_u(0) + k_d\bar{\varepsilon}_d$, $|w(t)| \leq \bar{w} := \rho_w(0) + k_z\bar{\varepsilon}_z$, $|r(t)| \leq \bar{r} := \rho_r(0) + k_o\bar{\varepsilon}_o$) as well as of the control signals (38)-(40) (i.e., $|X(t)| \leq k_u\bar{\varepsilon}_u$, $|Z(t)| \leq k_w\bar{\varepsilon}_w$, $|N(t)| \leq k_r\bar{\varepsilon}_r$) for all $t \in [0, \tau_{\max})$. Moreover, applying the inverse logarithmic function, we obtain:

$$-1 < \frac{\exp(-\bar{\varepsilon}_i)-1}{\exp(-\bar{\varepsilon}_i)+1} = \underline{\xi_i} \leq \xi_i(t) \leq \overline{\xi_i} = \frac{\exp(\bar{\varepsilon}_i)-1}{\exp(\bar{\varepsilon}_i)+1} < 1 \quad (59)$$

for all $i \in \{d, z, o, u, w, r\}$. Finally, linearizing around the origin the dynamics of the unactuated degrees of freedom $\boldsymbol{s}$ defined in (8), (10), (12) and (13), we obtain:

$$\dot{\boldsymbol{s}} = A\boldsymbol{s} + g(t, \boldsymbol{s}, u, w, r)$$

where

$$A = \mathrm{diag}\left(\frac{Y_v}{m_v}, \begin{bmatrix} 0 & 1 \\ \frac{z_B W}{m_p} & \frac{K_p}{m_p} \end{bmatrix}, \begin{bmatrix} 0 & 1 \\ \frac{z_B W}{m_q} & \frac{M_q}{m_q} \end{bmatrix}\right)$$

and $g(t, \boldsymbol{s}, u, w, r)$ is a perturbation term, that is continuous in t and locally Lipschitz in $\boldsymbol{s}$, u, w, r on $\Omega_{\boldsymbol{s}}$, $\Omega_u = \{u \in \Re : |u| \leq \bar{u}\}$, $\Omega_w = \{w \in \Re : |w| \leq \bar{w}\}$ and $\Omega_r = \{r \in \Re : |r| \leq \bar{r}\}$. Notice that the model parameters Y_v, K_p, M_q, z_B are negative whereas m_v, m_p, m_q, W are positive. Hence, the diagonal elements of A are Hurwitz matrices. Therefore, A is also a Hurwitz matrix and consequently, owing to the Lyapunov equation, there exist positive definite matrices P, Q such that $PA + A^TP = -Q$. Moreover, owing to the boundedness of the disturbance terms $\delta_v(t)$, $\delta_p(t)$ and $\delta_q(t)$ for all $t \geq 0$ and the fact that $\Omega_{\boldsymbol{s}}$, Ω_u, Ω_w and Ω_r are compact sets, the application of the Extreme Value Theorem guarantees the existence of a positive constant $\bar{g}$, independent of $\tau_{\max}$, such that $\|g(t, \boldsymbol{s}, u, w, r)\| \leq \bar{g}$, for all $(t, \boldsymbol{s}, u, w, r) \in [0, \tau_{\max}) \times \Omega_s \times \Omega_u \times \Omega_w \times \Omega_r$. Thus, adopting the positive definite function $V_s = \frac{1}{2}s^TPs$ and invoking [41] (Theorem 4.10 in p. 202), we conclude that $\boldsymbol{s}(t) \in \Omega_{\boldsymbol{s}}^{'}$, $\forall t \in [0, \tau_{\max})$, where:

$$\Omega_{\boldsymbol{s}}^{'} = \left\{\boldsymbol{s} \in \Re^3 : \|\boldsymbol{s}\| \leq \bar{\boldsymbol{s}}^{'} := \max\left\{\|\boldsymbol{s}(0)\|, \frac{\bar{g}\sqrt{\frac{\lambda_{\max}(P)}{\lambda_{\min}(P)}}}{\lambda_{\min}(Q)}\right\}\right\} \quad (60)$$

is a compact set, the size of which depends on: i) the control gain values k_d, k_z, k_o, ii) the control parameters $\rho_u(0)$, $\rho_w(0)$, $\rho_r(0)$, iii) the magnitude of the external disturbances, iv) the desired trajectory and v) the transient performance specifications, that all affect the size of $\bar{g}$ as well as on vi) the parameters of the dynamic model (9)-(14) that affect the positive definite matrices P and Q.

Notice also that (59) and (60) imply that $\boldsymbol{\xi}(t) \in \Omega_{\boldsymbol{\xi}}^{'} := \prod_{i \in \{d,z,o,u,w,r\}} \left[\frac{e^{-\bar{\varepsilon}_i}-1}{e^{-\bar{\varepsilon}_i}+1}, \frac{e^{\bar{\varepsilon}_i}-1}{e^{\bar{\varepsilon}_i}+1}\right] \times \Omega_{\boldsymbol{s}}^{'}$, $\forall t \in [0, \tau_{\max})$. Moreover, it can be easily verified that $\Omega_{\boldsymbol{\xi}}^{'} \subset \Omega_{\boldsymbol{\xi}}$ for certain, sufficient small control gain values k_d, k_z, k_o and parameters $\rho_u(0)$, $\rho_w(0)$, $\rho_r(0)$ satisfying $\bar{\boldsymbol{s}}^{'} < \bar{\boldsymbol{s}}$, which based on Proposition 1 further dictates $\tau_{\max} = \infty$. As a result, all closed loop signals remain bounded and moreover $\boldsymbol{\xi}(t) \in \Omega_{\boldsymbol{\xi}}^{'} \subset \Omega_{\boldsymbol{\xi}}$, $\forall t \geq 0$. Finally, from (59), we conclude that:

$$\begin{aligned} \underline{\rho}_d < \frac{\exp(-\bar{\varepsilon}_d)-1}{\exp(-\bar{\varepsilon}_d)+1}\frac{\rho_d(t)-\underline{\rho}_d}{2} + \frac{\rho_d(t)+\underline{\rho}_d}{2} \\ \leq e_d(t) \leq \\ \frac{\exp(\bar{\varepsilon}_d)-1}{\exp(\bar{\varepsilon}_d)+1}\frac{\rho_d(t)-\underline{\rho}_d}{2} + \frac{\rho_d(t)+\underline{\rho}_d}{2} < \rho_d(t) \\ -\rho_z(t) < \frac{\exp(-\bar{\varepsilon}_z)-1}{\exp(-\bar{\varepsilon}_z)+1}\rho_z(t) \leq e_z(t) \leq \frac{\exp(\bar{\varepsilon}_z)-1}{\exp(\bar{\varepsilon}_z)+1}\rho_z(t) < \rho_z(t) \\ -\rho_o(t) < \frac{\exp(-\bar{\varepsilon}_o)-1}{\exp(-\bar{\varepsilon}_o)+1}\rho_o(t) \leq e_o(t) \leq \frac{\exp(\bar{\varepsilon}_o)-1}{\exp(\bar{\varepsilon}_o)+1}\rho_o(t) < \rho_o(t) \end{aligned}$$

for all $t \geq 0$ and consequently the solution of the robust prescribed performance tracking control problem as stated in Subsection II-C, which completes the proof.

REFERENCES

[1] C. P. Bechlioulis and G. A. Rovithakis, "Robust partial-state feedback prescribed performance control of cascade systems with unknown nonlinearities," *IEEE Transactions on Automatic Control*, vol. 56, no. 9, pp. 2224–2230, 2011.

[2] ——, "A low-complexity global approximation-free control scheme with prescribed performance for unknown pure feedback systems," *Automatica*, vol. 50, no. 4, pp. 1217–1226, 2014.

[3] T. I. Fossen, *Guidance and control of ocean vehicles*. Chichester, U.K.: John Wiley & Sons Ltd., 1994.

[4] T. J. Koo and S. Sastry, "Output tracking control design of a helicopter model based on approximate linearization," *Proceedings of the IEEE Conference on Decision and Control*, vol. 4, pp. 3635–3640, 1998.

[5] S. A. Al-Hiddabi and N. H. McClamroch, "Tracking and maneuver regulation control for nonlinear nonminimum phase systems: Application to flight control," *IEEE Transactions on Control Systems Technology*, vol. 10, no. 6, pp. 780–792, 2002.

[6] J. R. T. Lawton, R. W. Beard, and B. J. Young, "A decentralized approach to formation maneuvers," *IEEE Transactions on Robotics and Automation*, vol. 19, no. 6, pp. 933–941, 2003.

[7] F. Alonge, F. D'Ippolito, and F. Raimondi, "Trajectory tracking of underactuated underwater vehicles," *Proceedings of the IEEE Conference on Decision and Control*, vol. 5, pp. 4421–4426, 2001.

[8] A. Aguiar and A. Pascoal, "Dynamic positioning and way-point tracking of underactuated auvs in the presence of ocean currents," *International Journal of Control*, vol. 80, no. 7, pp. 1092–1108, 2007.

[9] ——, "Dynamic positioning and way-point tracking of underactuated auvs in the presence of ocean currents," *Proceedings of the IEEE Conference on Decision and Control*, vol. 2, pp. 2105–2110, 2002.

[10] A. Aguiar and J. Hespanha, "Position tracking of underactuated vehicles," *Proceedings of the American Control Conference*, vol. 3, pp. 1988–1993, 2003.

[11] A. Baviskar, M. Feemster, D. Dawson, and B. Xian, "Tracking control of an underactuated unmanned underwater vehicle," *Proceedings of the American Control Conference*, vol. 6, pp. 4321–4326, 2005.

[12] F. Repoulias and E. Papadopoulos, "Planar trajectory planning and tracking control design for underactuated auvs," *Ocean Engineering*, vol. 34, no. 11-12, pp. 1650–1667, 2007.

[13] J. Refsnes, A. Srensen, and K. Pettersen, "Model-based output feedback control of slender-body underactuated auvs: Theory and experiments," *IEEE Transactions on Control Systems Technology*, vol. 16, no. 5, pp. 930–946, 2008.

[14] F. Bi, Y. Wei, J. Zhang, and W. Cao, "Position-tracking control of underactuated autonomous underwater vehicles in the presence of unknown ocean currents," *IET Control Theory and Applications*, vol. 4, 2010.

[15] K. Do, "Global tracking control of underactuated odins in three-dimensional space," *International Journal of Control*, vol. 86, no. 2, pp. 183–196, 2013.

[16] X. Xiang, L. Lapierre, C. Liu, and B. Jouvencel, "Path tracking: Combined path following and trajectory tracking for autonomous underwater vehicles," *IEEE International Conference on Intelligent Robots and Systems*, pp. 3558–3563, 2011.

[17] P. Encarnao and A. Pascoal, "Combined trajectory tracking and path following: An application to the coordinated control of autonomous marine craft," *Proceedings of the IEEE Conference on Decision and Control*, vol. 1, pp. 964–969, 2001.

[18] A. Aguiar and J. Hespanha, "Trajectory-tracking and path-following of underactuated autonomous vehicles with parametric modeling uncertainty," *IEEE Transactions on Automatic Control*, vol. 52, no. 8, pp. 1362–1379, 2007.

[19] K. Do, J. Pan, and Z. Jiang, "Robust and adaptive path following for underactuated autonomous underwater vehicles," *Ocean Engineering*, vol. 31, no. 16, pp. 1967–1997, 2004.

[20] K. Do and J. Pan, "Robust and adaptive path following for underactuated autonomous underwater vehicles," *Proceedings of the American Control Conference*, vol. 3, pp. 1994–1999, 2003.

[21] G. Antonelli, S. Chiaverini, N. Sarkar, and M. West, "Adaptive control of an autonomous underwater vehicle: Experimental results on odin," *IEEE Transactions on Control Systems Technology*, vol. 9, no. 5, pp. 756–765, 2001.

[22] L. Lapierre and B. Jouvencel, "Robust nonlinear path-following control of an auv," *IEEE Journal of Oceanic Engineering*, vol. 33, no. 2, pp. 89–102, 2008.

[23] L. Lapierre, "Robust diving control of an auv," *Ocean Engineering*, vol. 36, no. 1, pp. 92–104, 2009.

[24] R. Cristi, F. A. Papoulias, and A. J. Healey, "Adaptive sliding mode control of autonomous underwater vehicles in the dive plane," *IEEE Journal of Oceanic Engineering*, vol. 15, no. 3, pp. 152–160, 1990.

[25] M. Santhakumar and T. Asokan, "Investigations on the hybrid tracking control of an underactuated autonomous underwater robot," *Advanced Robotics*, vol. 24, no. 11, pp. 1529–1556, 2010.

[26] H. Ashrafiuon, K. Muske, L. McNinch, and R. Soltan, "Sliding-mode tracking control of surface vessels," *IEEE Transactions on Industrial Electronics*, vol. 55, no. 11, pp. 4004–4012, 2008.

[27] R. Soltan, H. Ashrafiuon, and K. Muske, "State-dependent trajectory planning and tracking control of unmanned surface vessels," *Proceedings of the American Control Conference*, pp. 3597–3602, 2009.

[28] D. Zhu, X. Hua, and B. Sun, "A neurodynamics control strategy for real-time tracking control of autonomous underwater vehicles," *Journal of Navigation*, vol. 67, no. 1, pp. 113–127, 2014.

[29] B. Taheri and E. Richer, "Equidistance target-following controller for underactuated autonomous underwater vehicles," *International Journal of Intelligent Computing and Cybernetics*, vol. 6, no. 2, pp. 108–125, 2013.

[30] J. Li and P. Lee, "A neural network adaptive controller design for free-pitch-angle diving behavior of an autonomous underwater vehicle," *Robotics and Autonomous Systems*, vol. 52, no. 2-3, pp. 132–147, 2005.

[31] K. Ishii, T. Fujii, and T. Ura, "On-line adaptation method in a neural network based control system for auv's," *IEEE Journal of Oceanic Engineering*, vol. 20, no. 3, pp. 221–228, 1995.

[32] B. Seok Park, "Neural network-based tracking control of underactuated autonomous underwater vehicles with model uncertainties," *Journal of Dynamic Systems, Measurement and Control, Transactions of the ASME*, vol. 137, no. 2, 2015.

[33] F. Raimondi and M. Melluso, "Hierarchical fuzzy/lyapunov control for horizontal plane trajectory tracking of underactuated auv," *IEEE International Symposium on Industrial Electronics*, pp. 1875–1882, 2010.

[34] F. Song and S. M. Smith, "Design of sliding mode fuzzy controllers for an autonomous underwater vehicle without system model," *Oceans Conference Record (IEEE)*, vol. 2, pp. 835–840, 2000.

[35] J. Guo, F.-C. Chiu, and C.-C. Huang, "Design of a sliding mode fuzzy controller for the guidance and control of an autonomous underwater vehicle," *Ocean Engineering*, vol. 30, no. 16, pp. 2137–2155, 2003.

[36] C. P. Bechlioulis and K. J. Kyriakopoulos, "Robust prescribed performance tracking control for unknown underactuated torpedo-like auvs," in *Proceedings of the European Control Conference*, 2013, pp. 4388–4393.

[37] E. D. Sontag, *Mathematical Control Theory*. London, U.K.: Springer, 1998.

[38] H. Xu and P. A. Ioannou, "Robust adaptive control for a class of mimo nonlinear systems with guaranteed error bounds," *IEEE Transactions on Automatic Control*, vol. 48, no. 5, pp. 728–742, 2003.

[39] K. Y. Pettersen and O. Egeland, "Time-varying exponential stabilization of the position and attitude of an underactuated autonomous underwater vehicle," *IEEE Transactions on Automatic Control*, vol. 44, no. 1, pp. 112–115, 1999.

[40] M. Prats, J. Perez, J. J. Fernandez, and P. J. Sanz, "An open source tool for simulation and supervision of underwater intervention missions," in *IEEE International Conference on Intelligent Robots and Systems*, 2012, pp. 2577–2582.

[41] H. K. Khalil, *Nonlinear Systems*. New York, U.S.A.: Mackmillan, 1992.